Bio-patterns

18.S995 - L12

dunkel@mit.edu

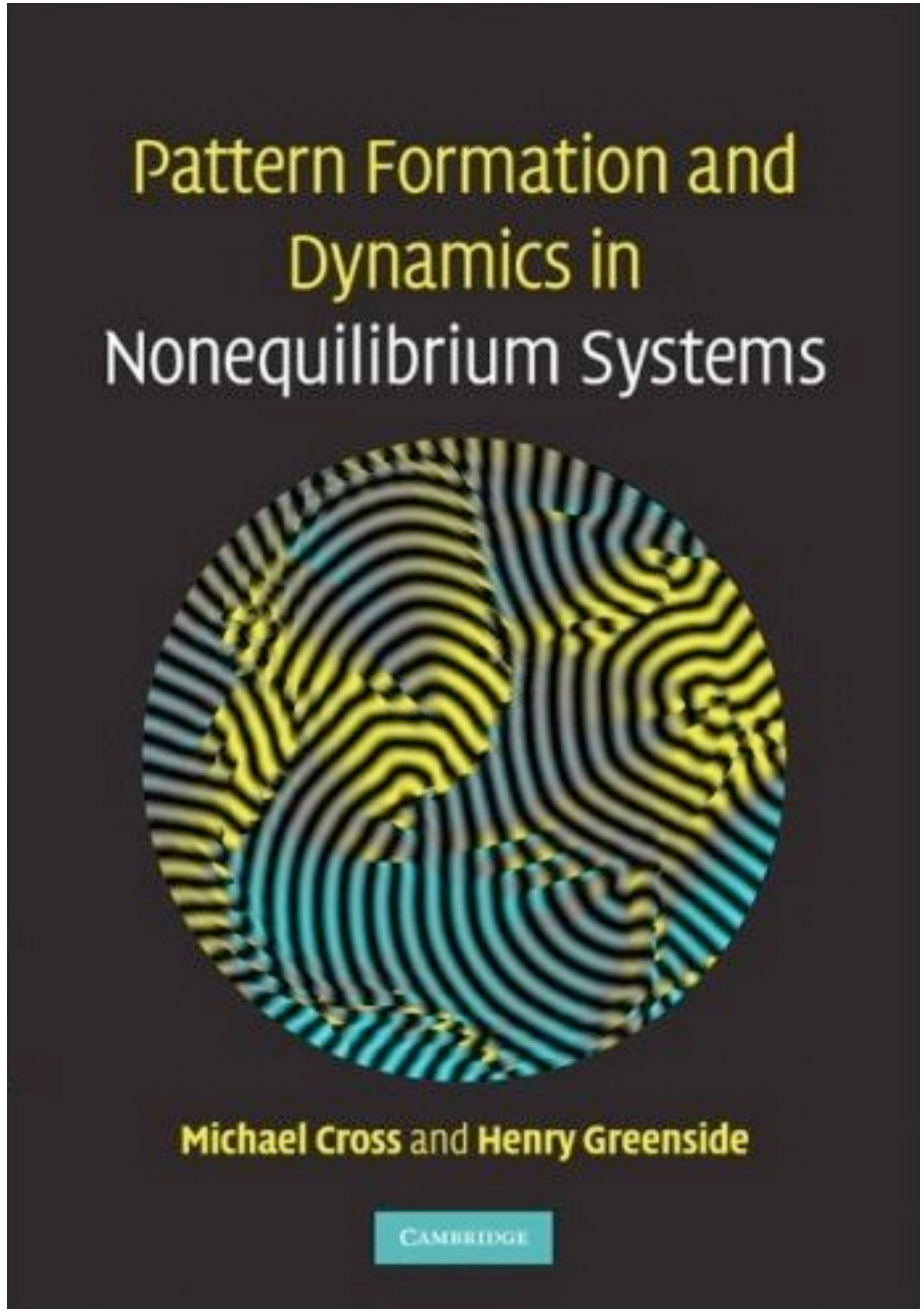

dunkel@math.mit.edu

Plankton

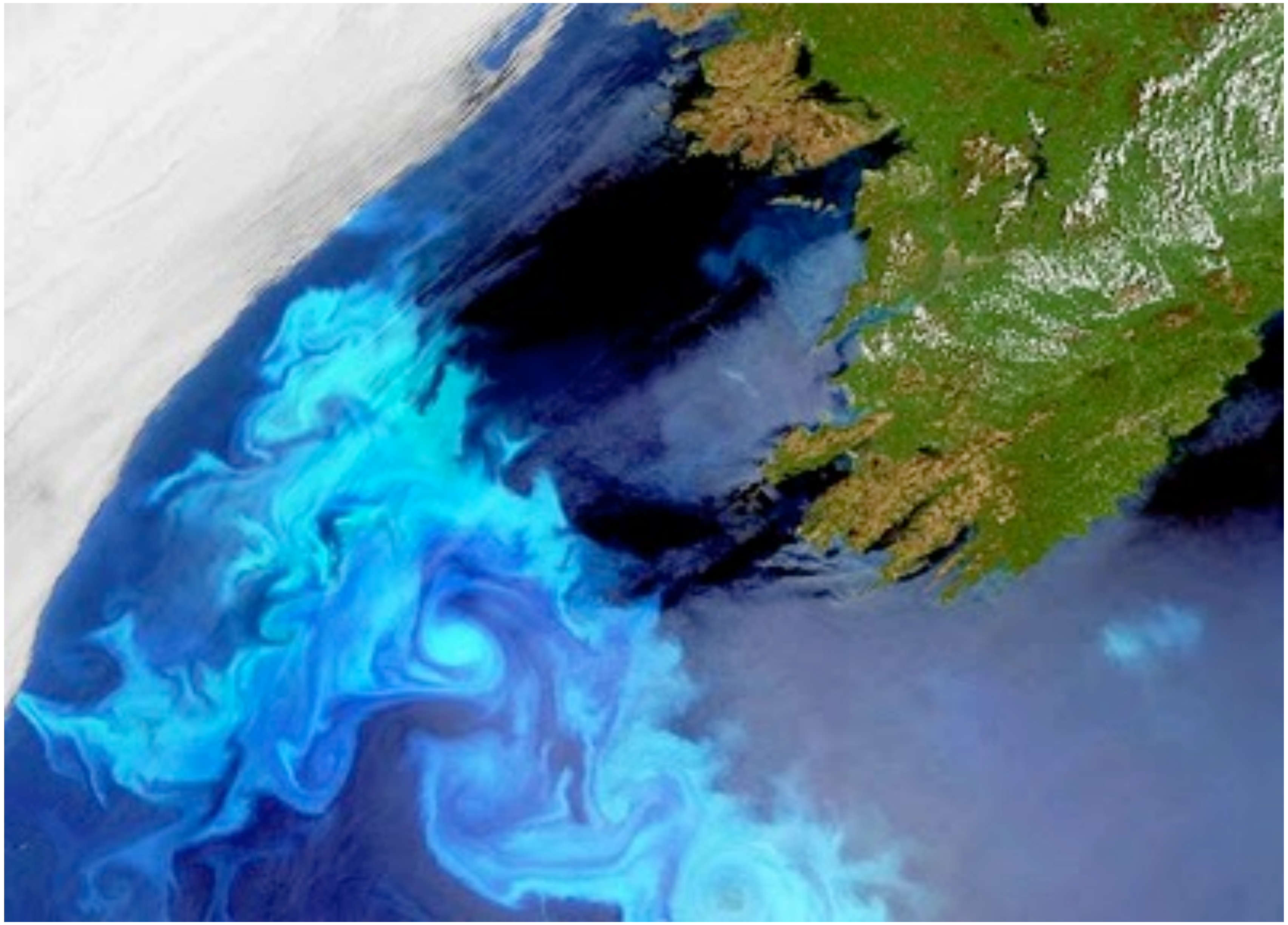

ESA cost of Ireland

dunkel@math.mit.edu

Animals

Shells

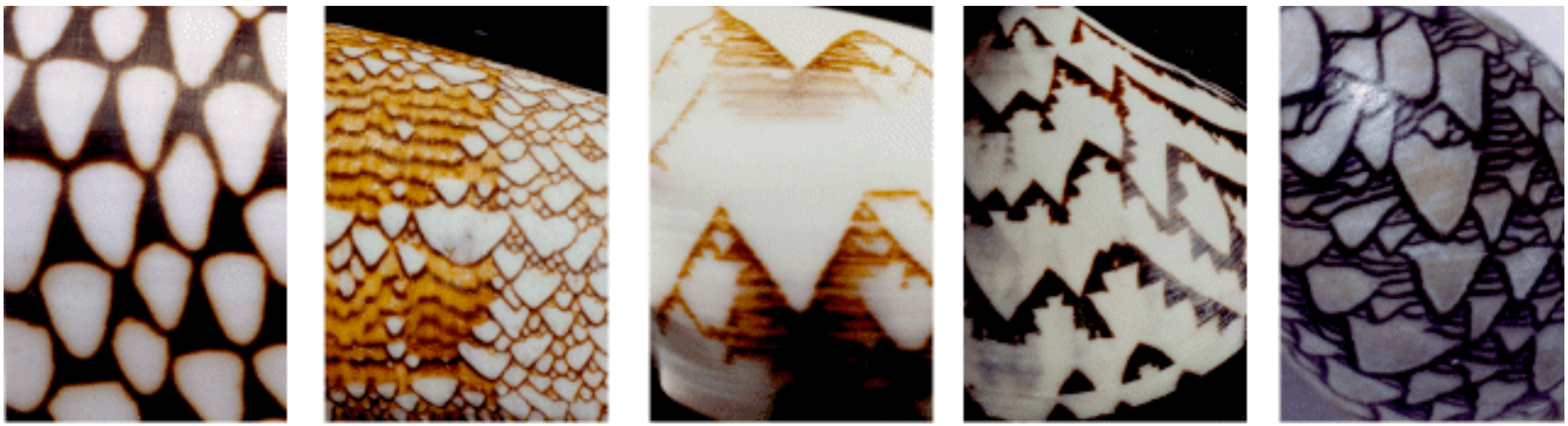

dunkel@math.mit.edu

Compare: vibrated granular media

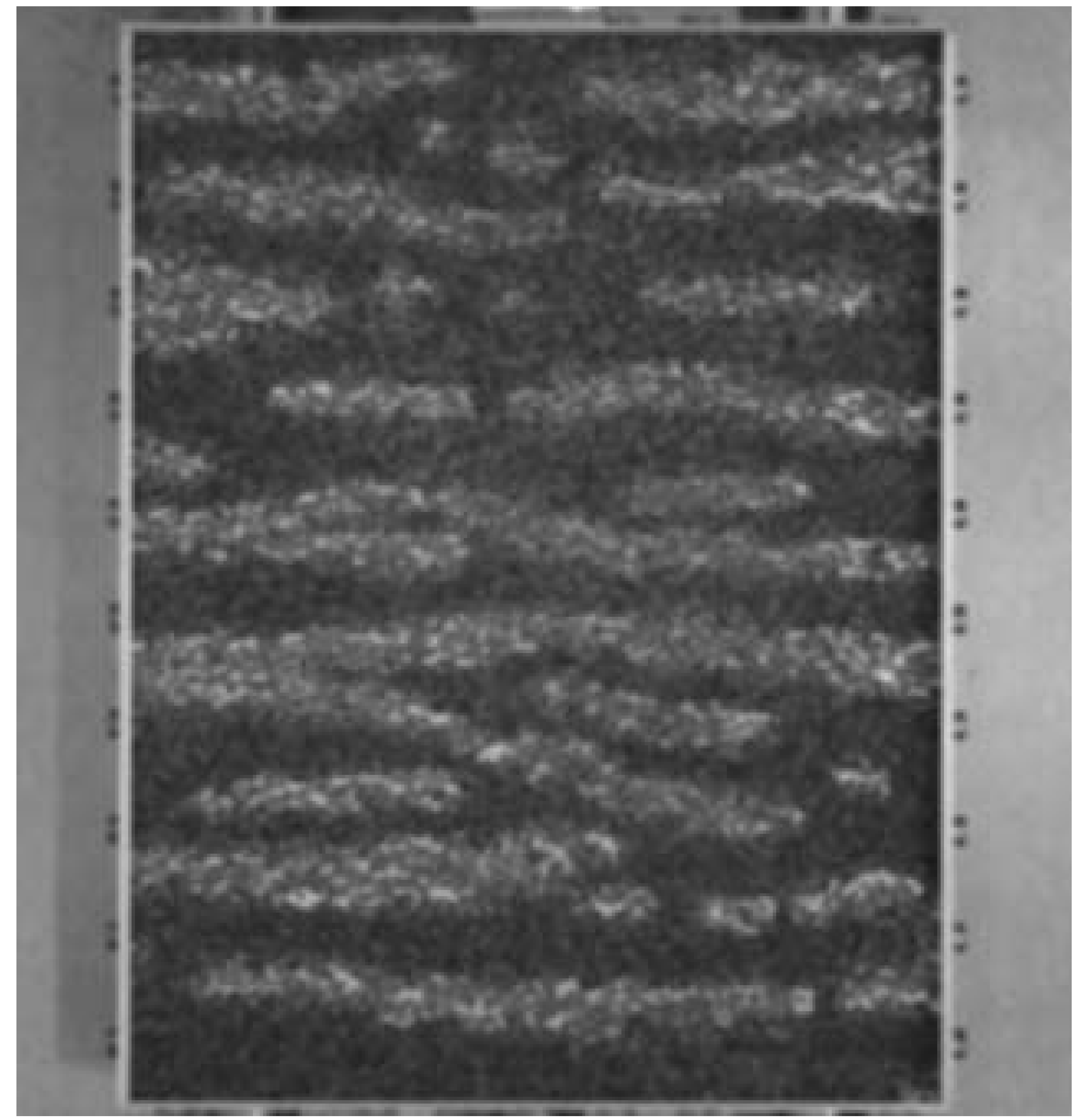

dunkel@math.mit.edu

Compare: vibrated granular media

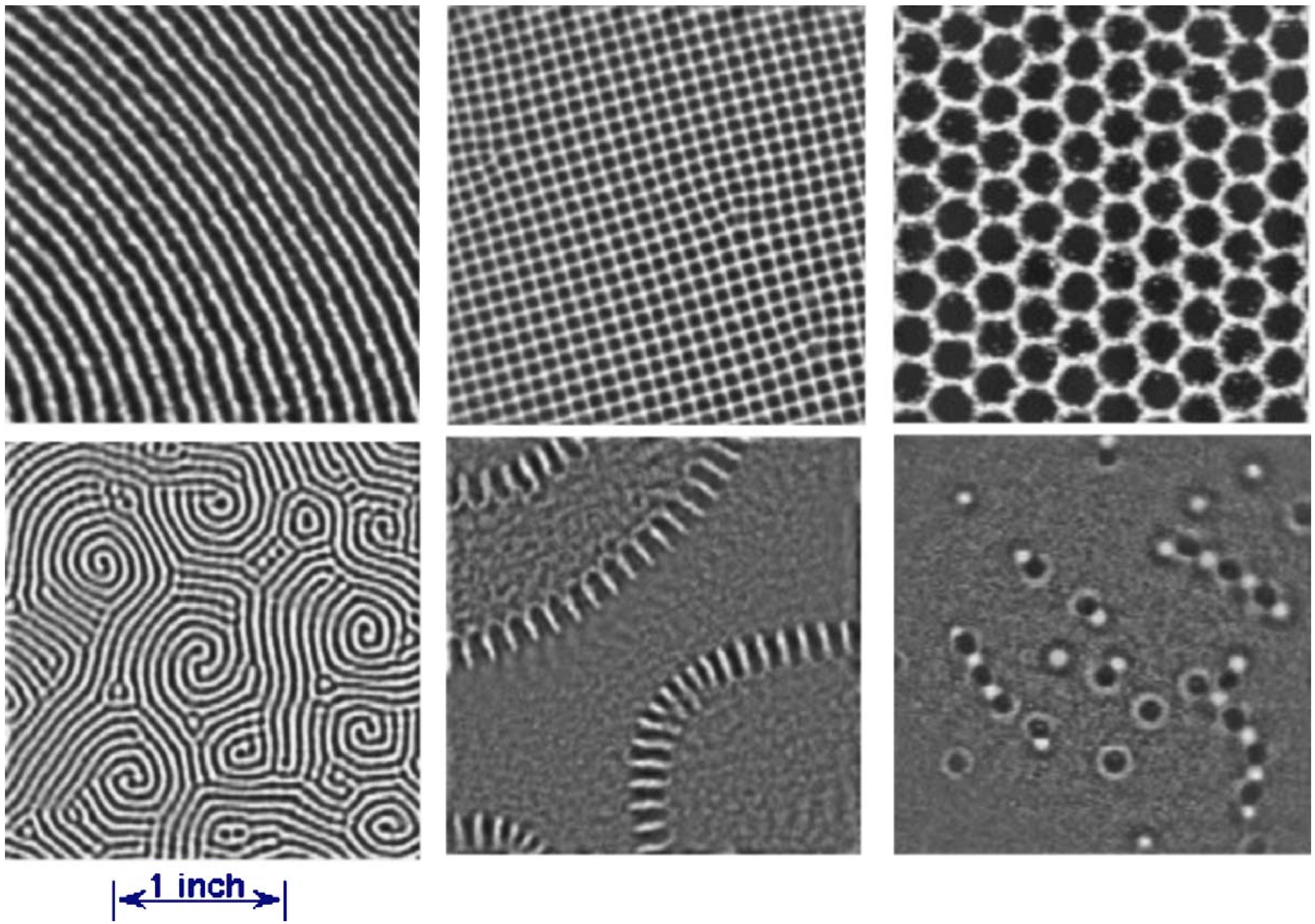

Slime mold

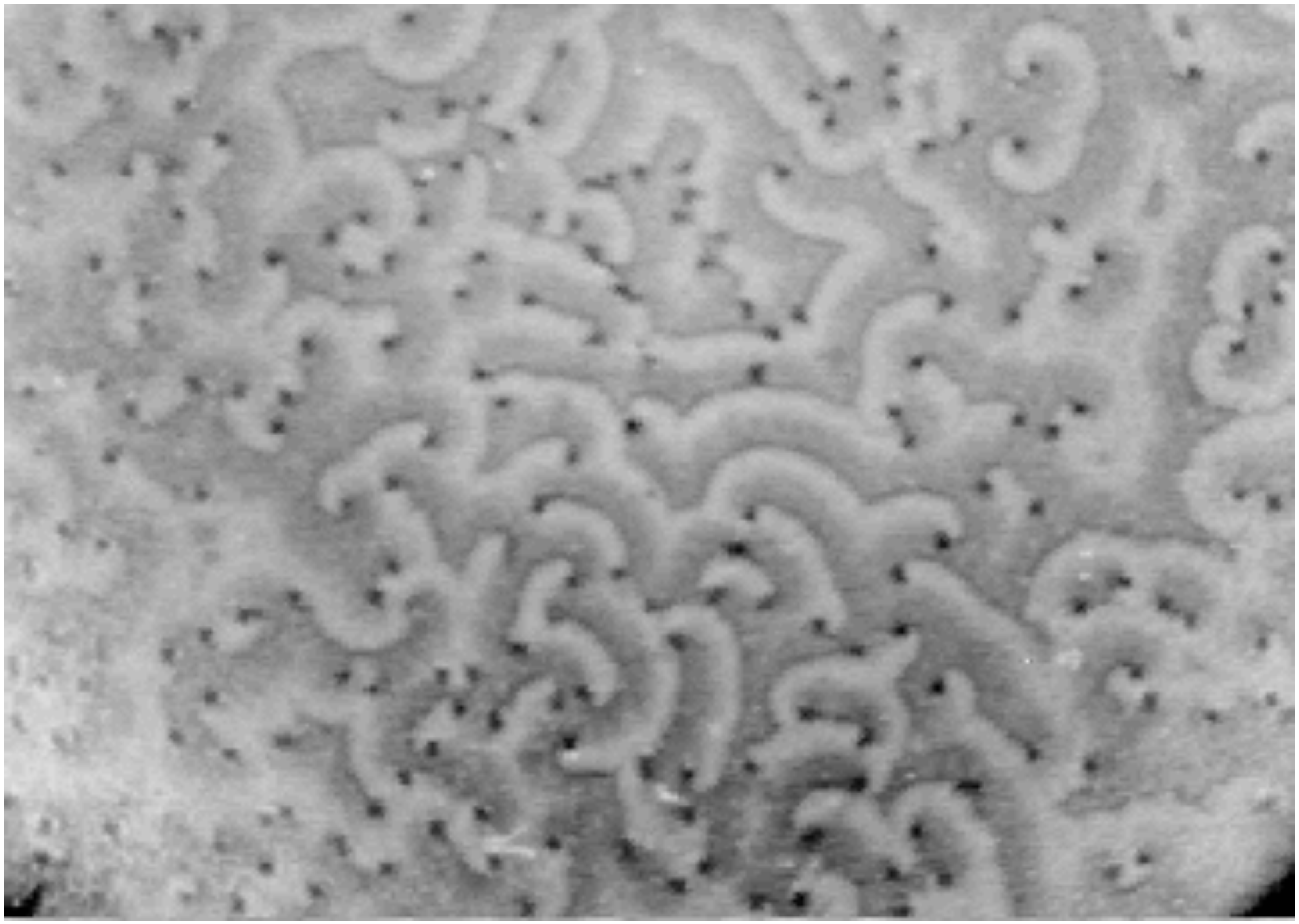

aggregation of a starving slime mold (credit: Florian Siegert)

dunkel@math.mit.edu

Belousov-Zhabotinsky reaction

Mix of potassium bromate, cerium(IV) sulfate, malonic acid and citric acid in dilute sulfuric acid

the ratio of concentration of the cerium(IV) and cerium(III) ions oscillated

This is due to the cerium(IV) ions being reduced by malonic acid to cerium(III) ions, which are then oxidized back to cerium(IV) ions by bromate(V) ions

dunkel@math.mit.edu

2d Swift-Hohenberg model

arxiv: 1208.4464

Sea urchin sperm cells
near surface
(high concentration)

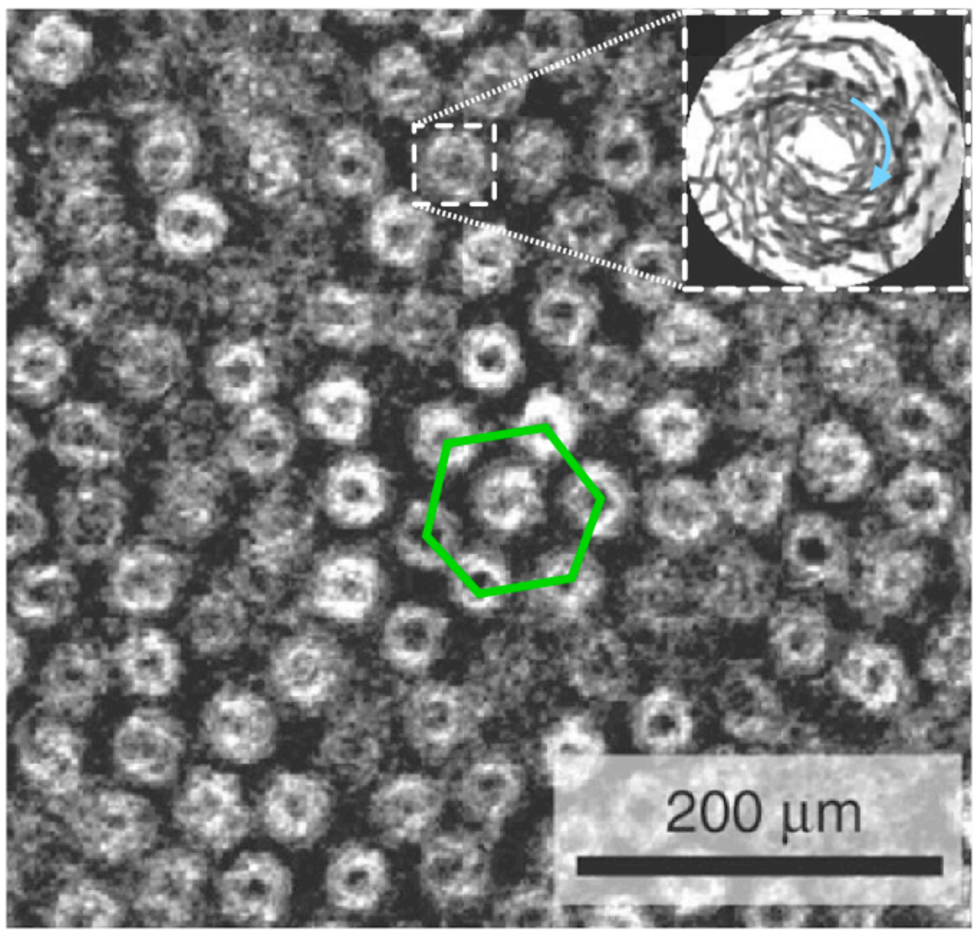

Riedel et al (2007) Science

broken
reflection-symmetry

$b \neq 0$

$\psi \not\mapsto -\psi$

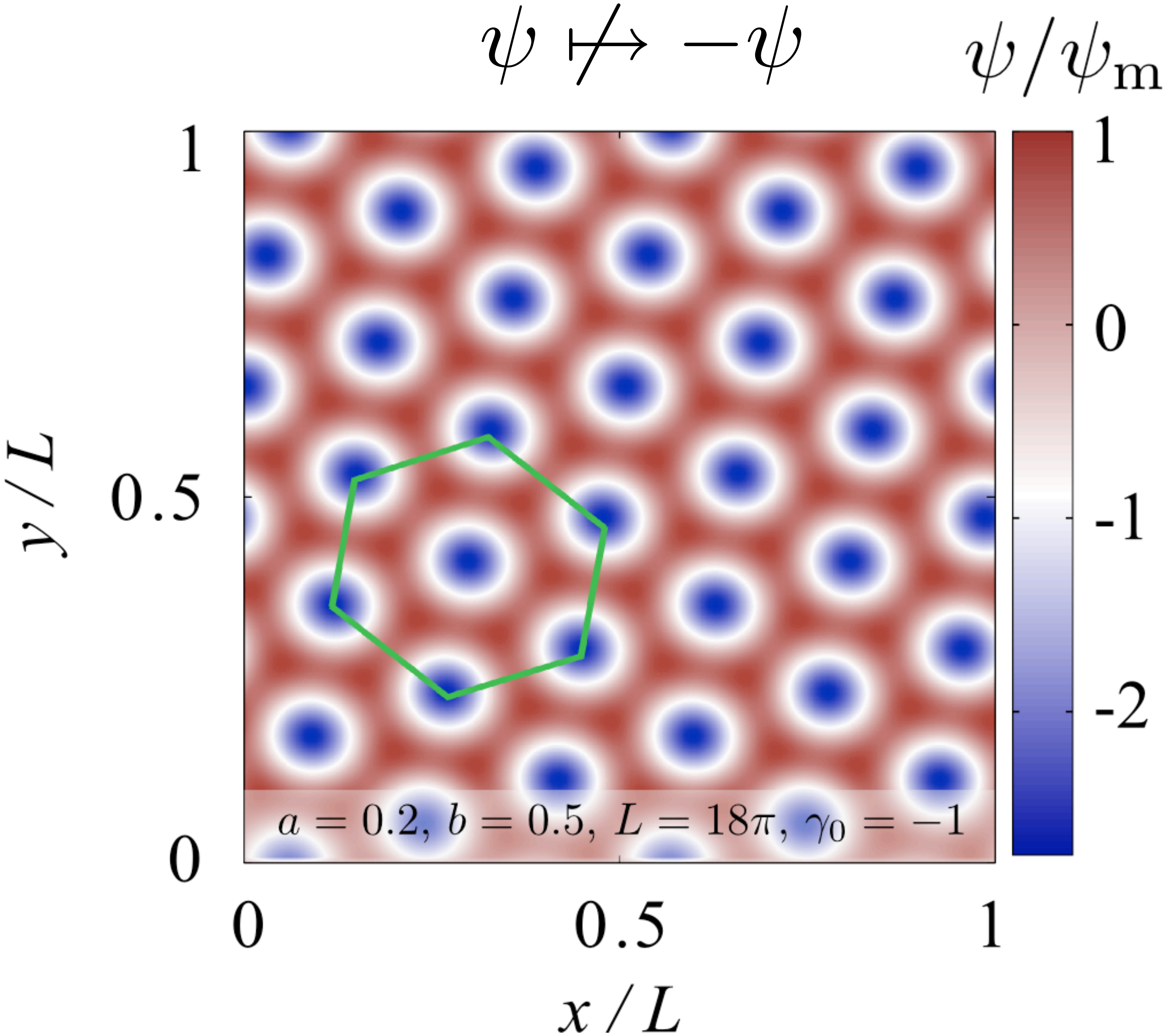

3D suspension

PRL (2013)

B. subtilis

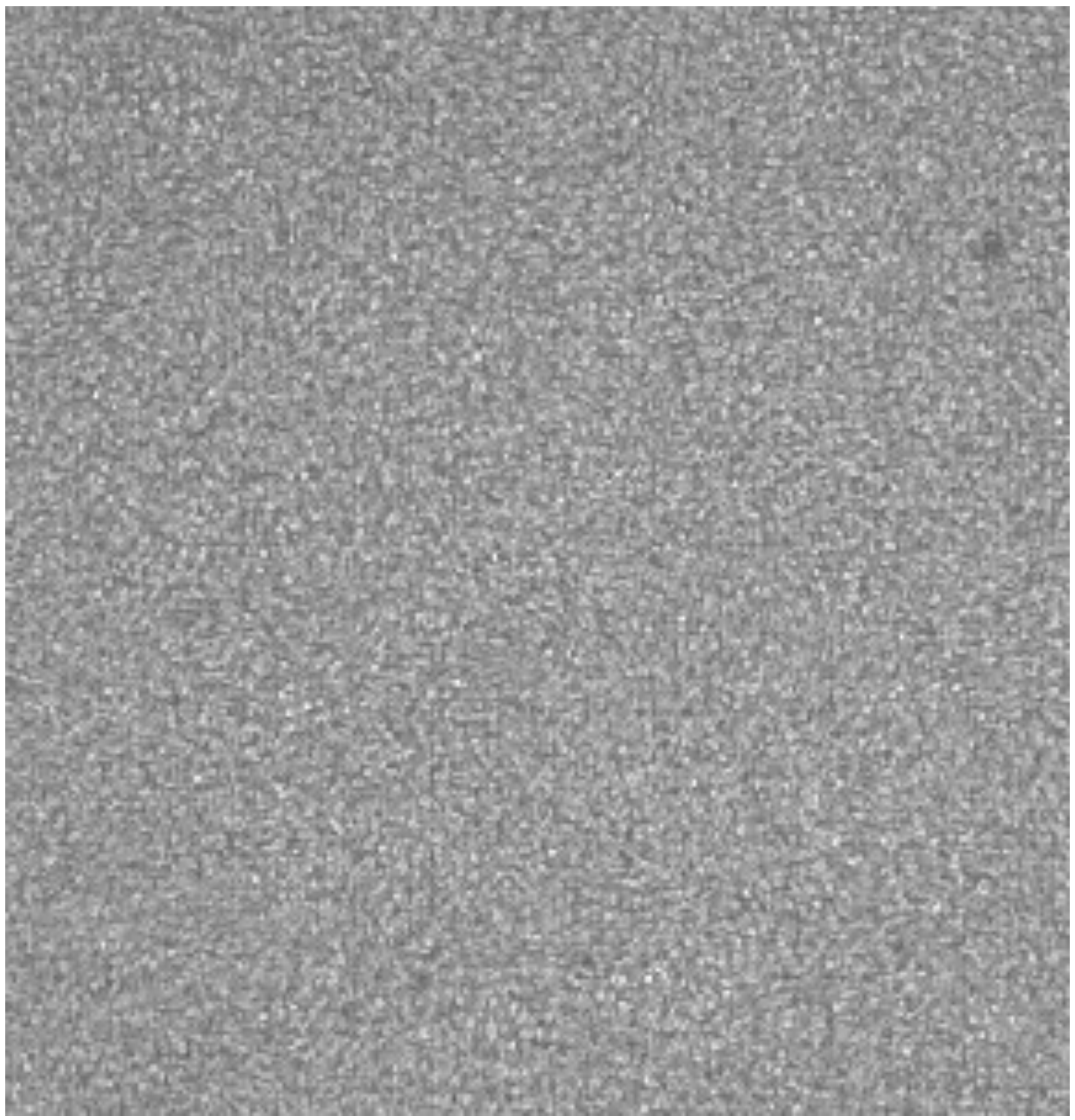

bright field

tracer

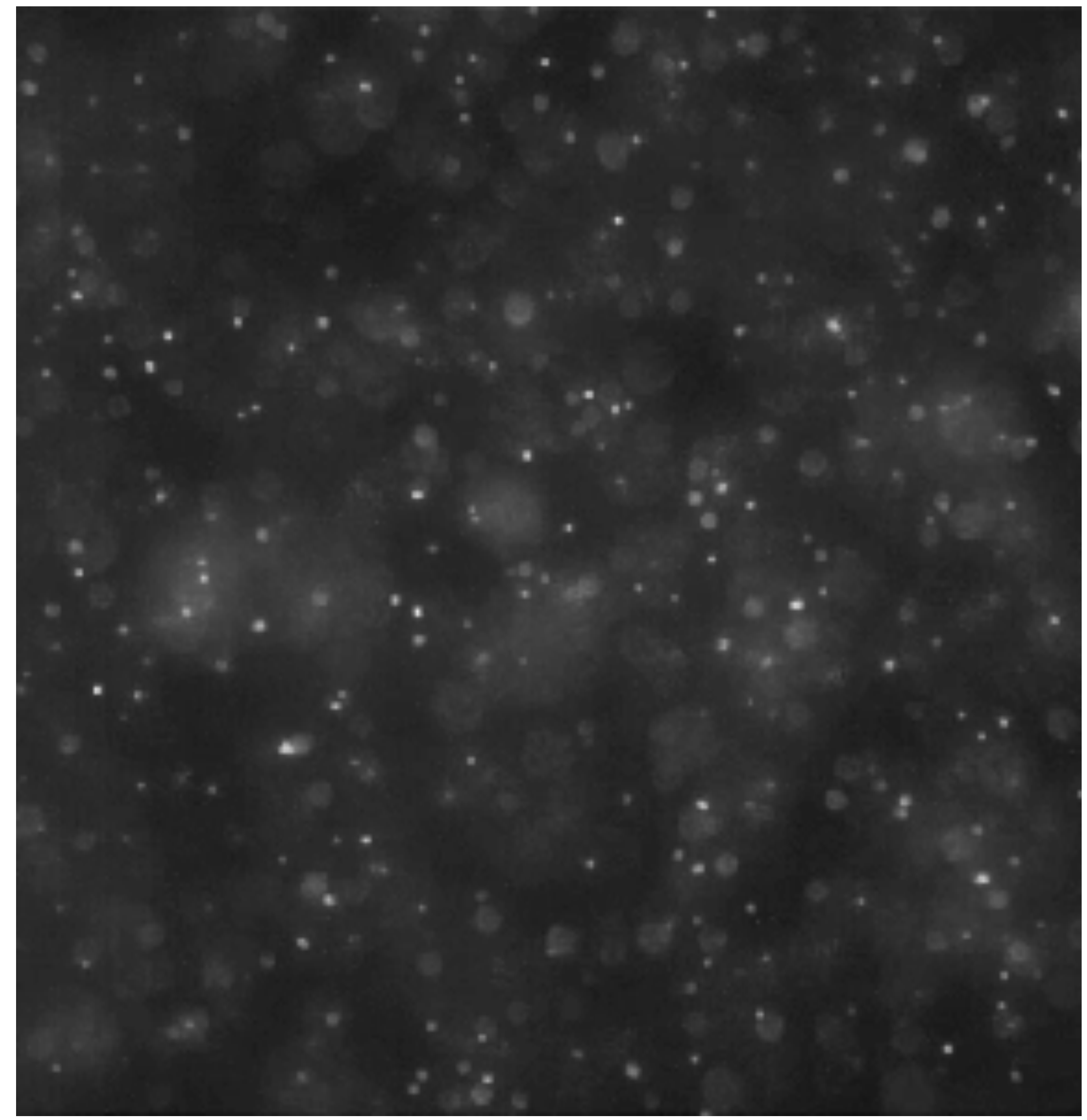

fluorescence

3D suspension

PRL (2013)

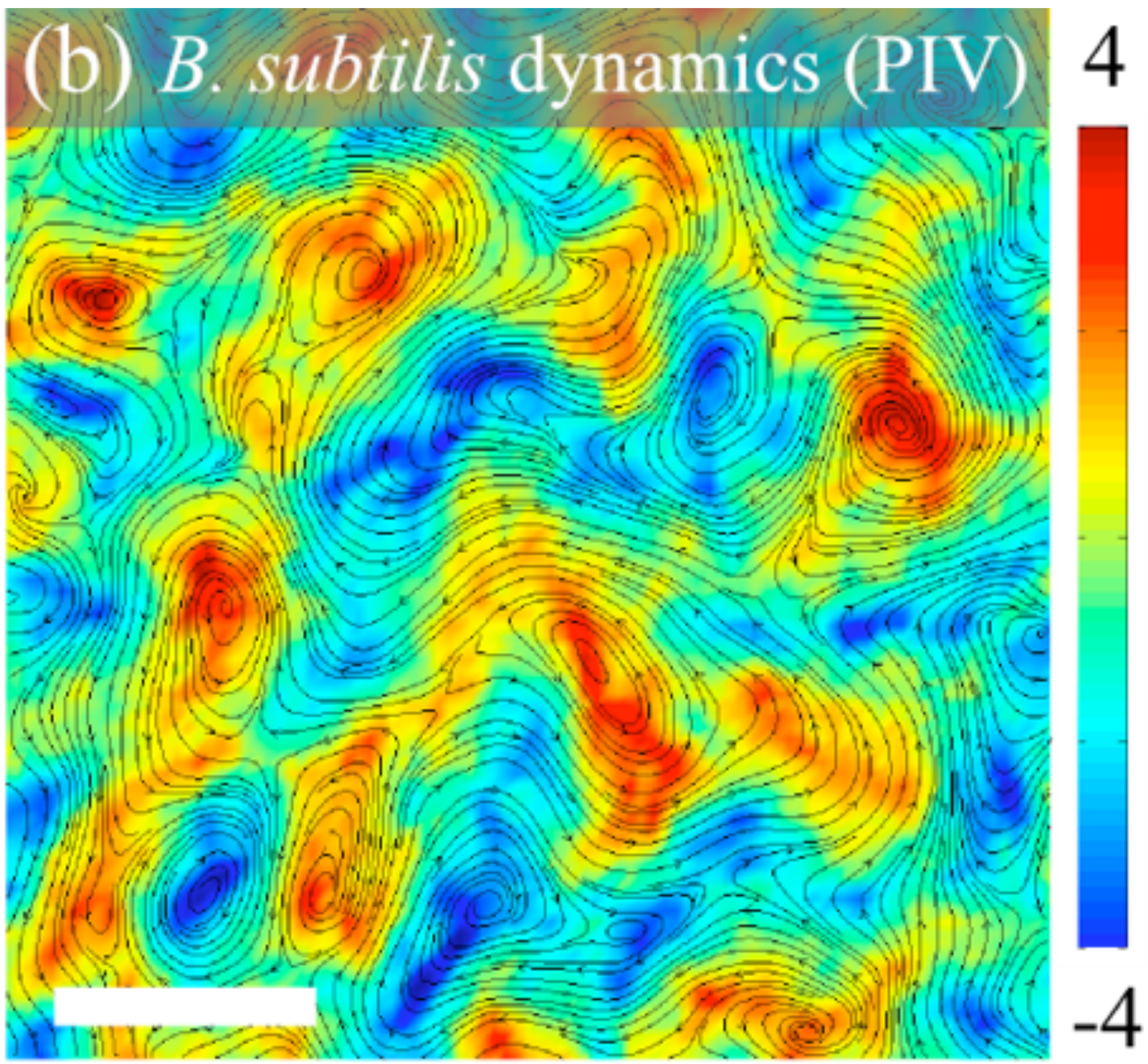

bright field

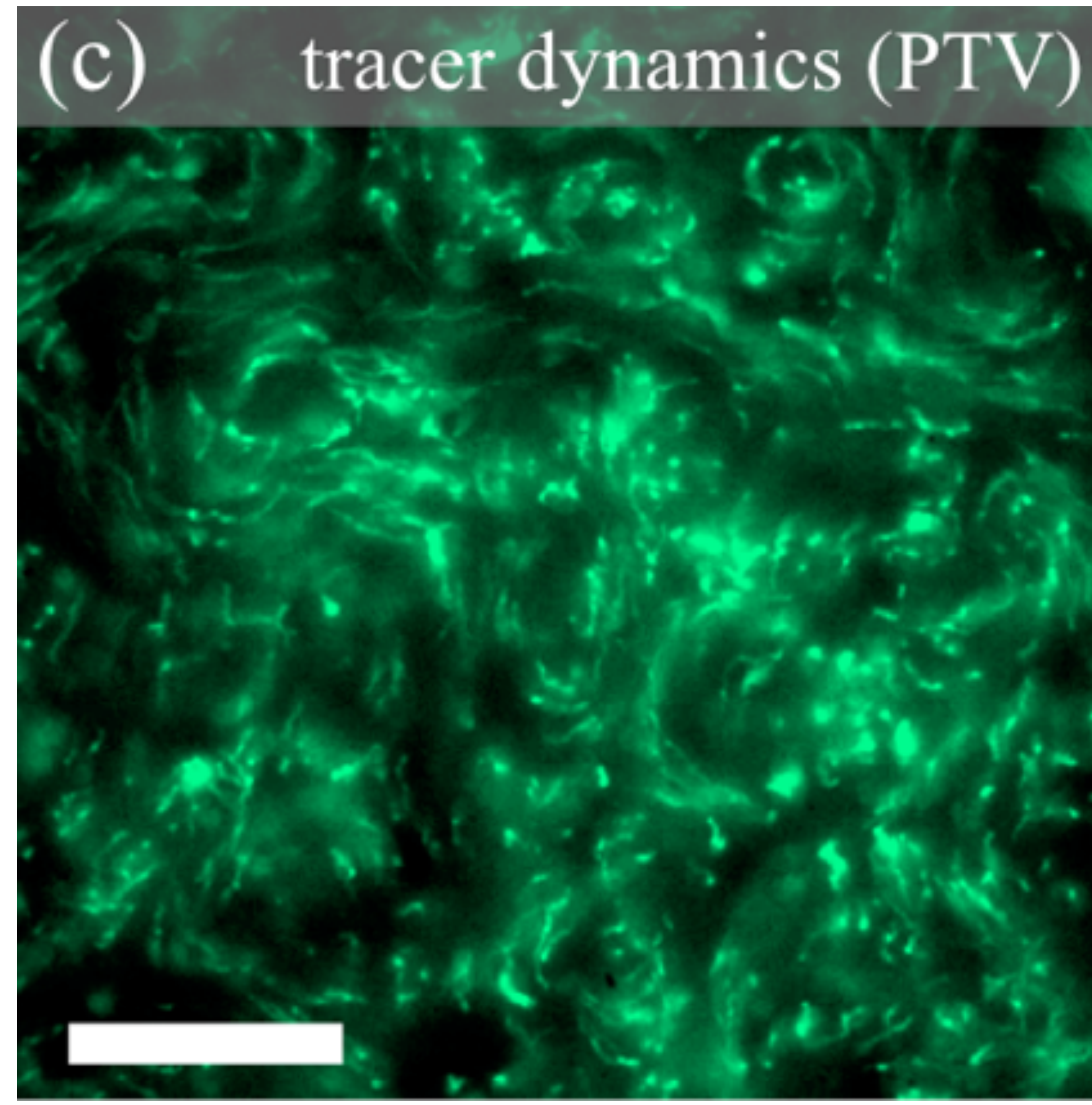

fluorescence

3D suspension

PRL (2013)

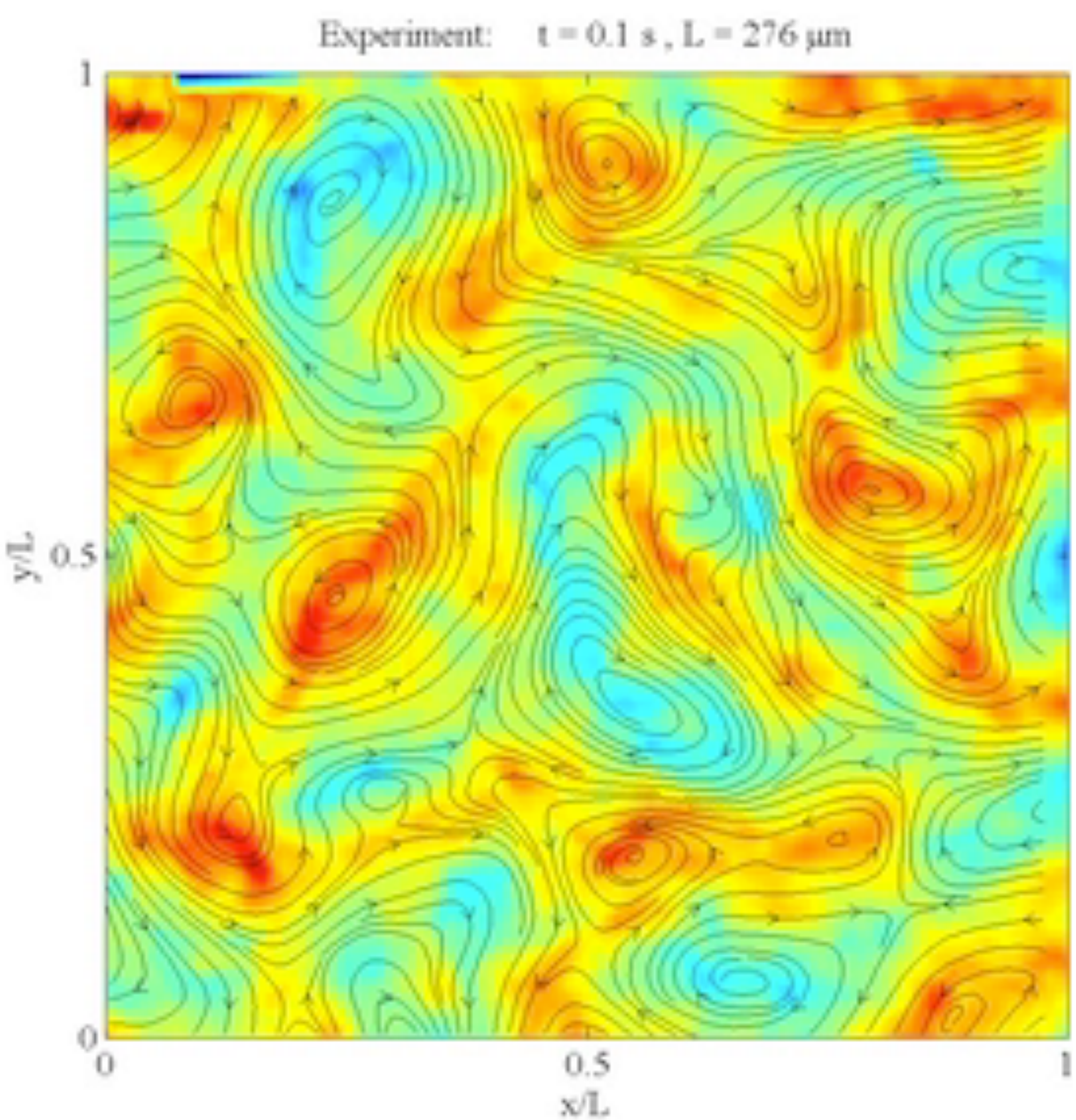

Experiment:
quasi-2D slice

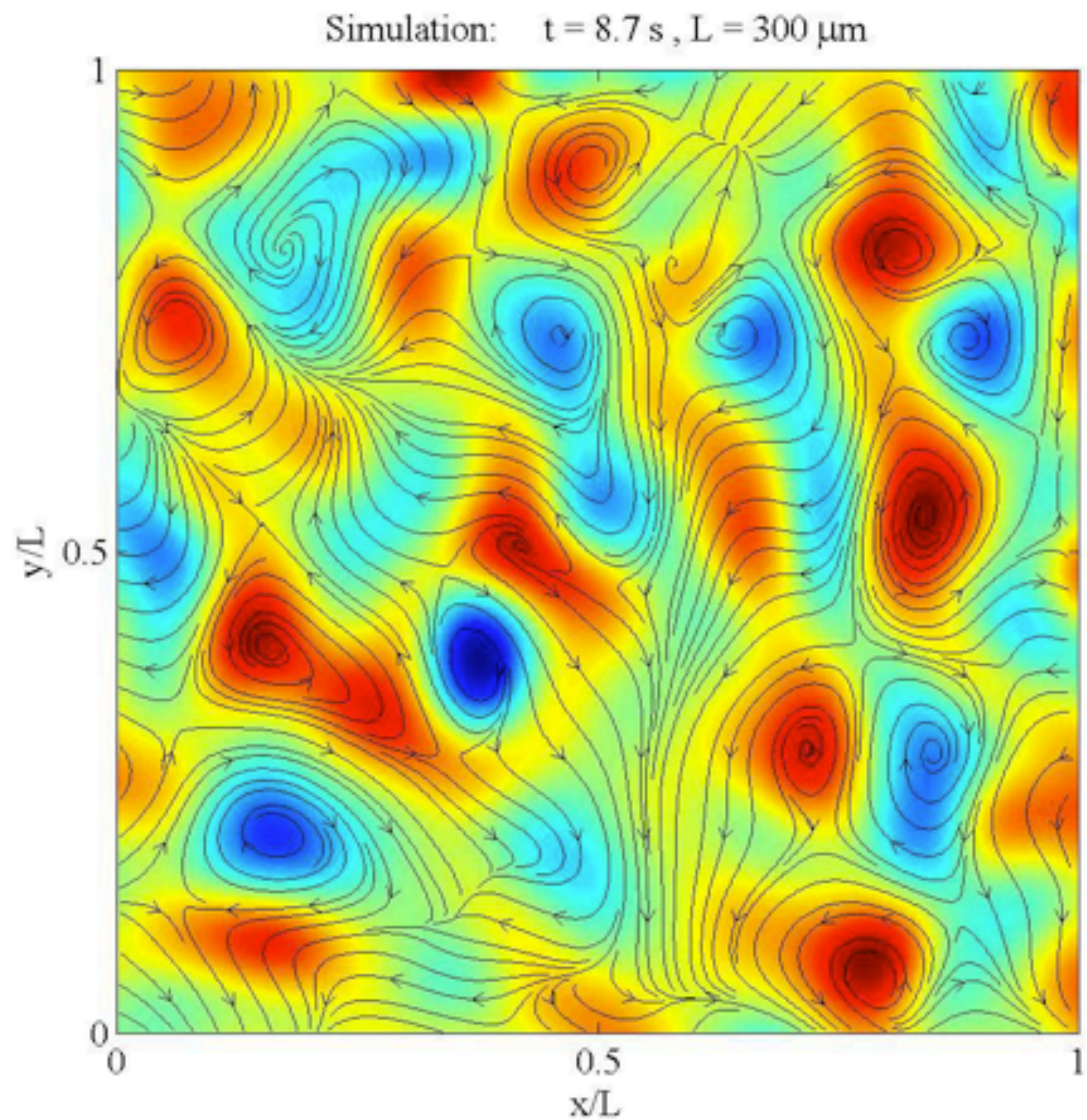

Theory:
2D slice

2D active nematics

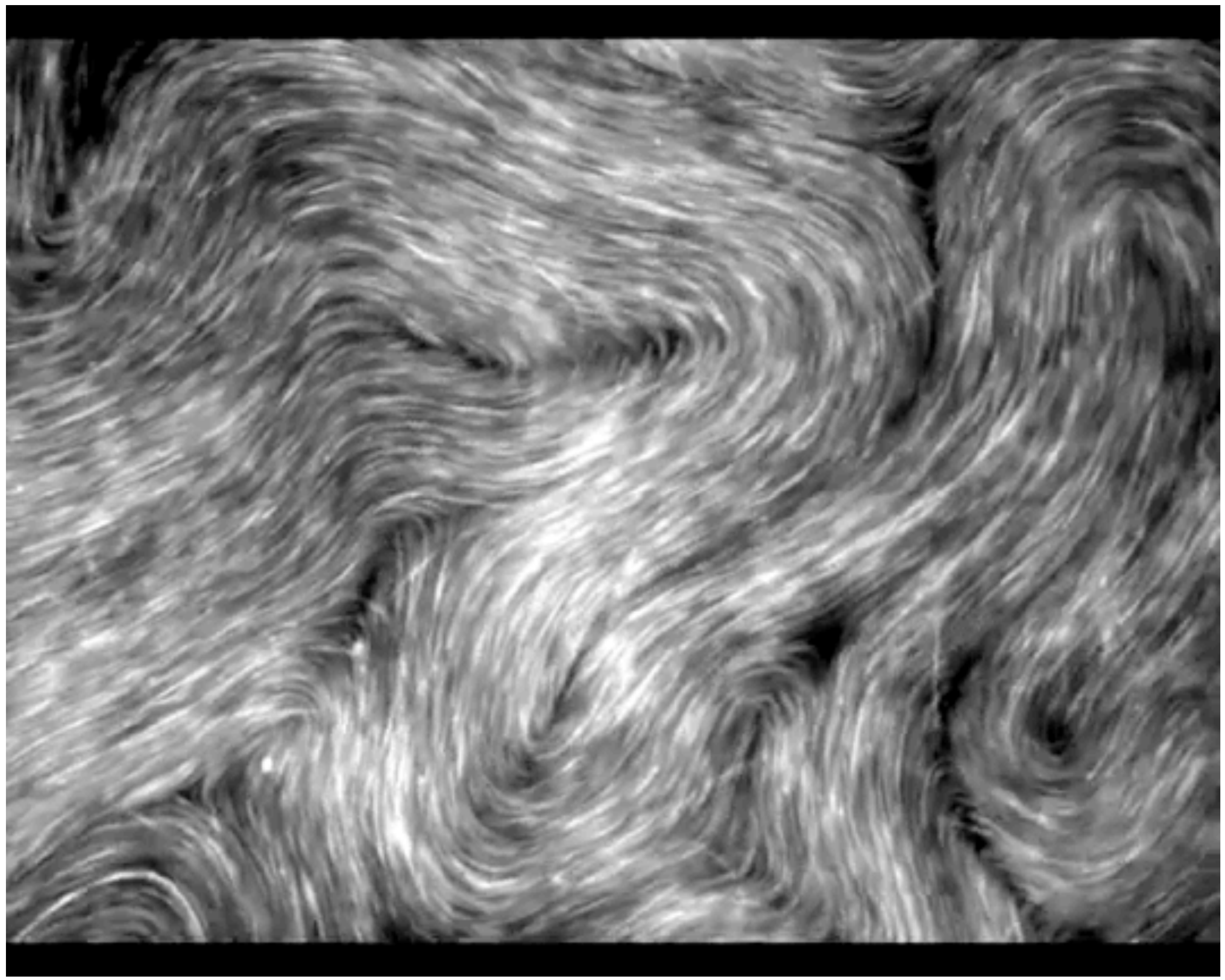

Dogic Lab Brandeis

dunkel@math.mit.edu

2D active nematics

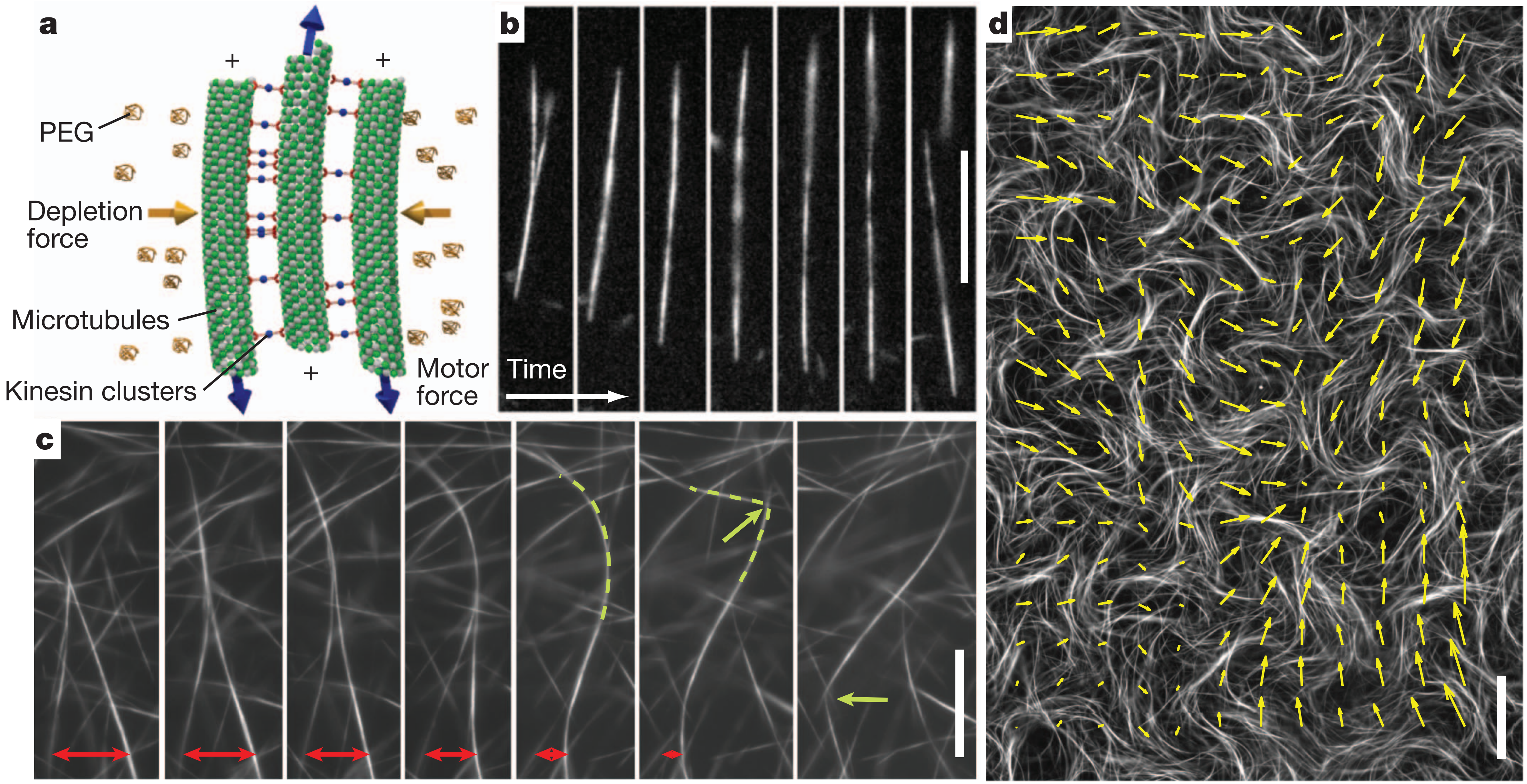

Dogic Lab Brandeis, Science 2012

2D active nematics

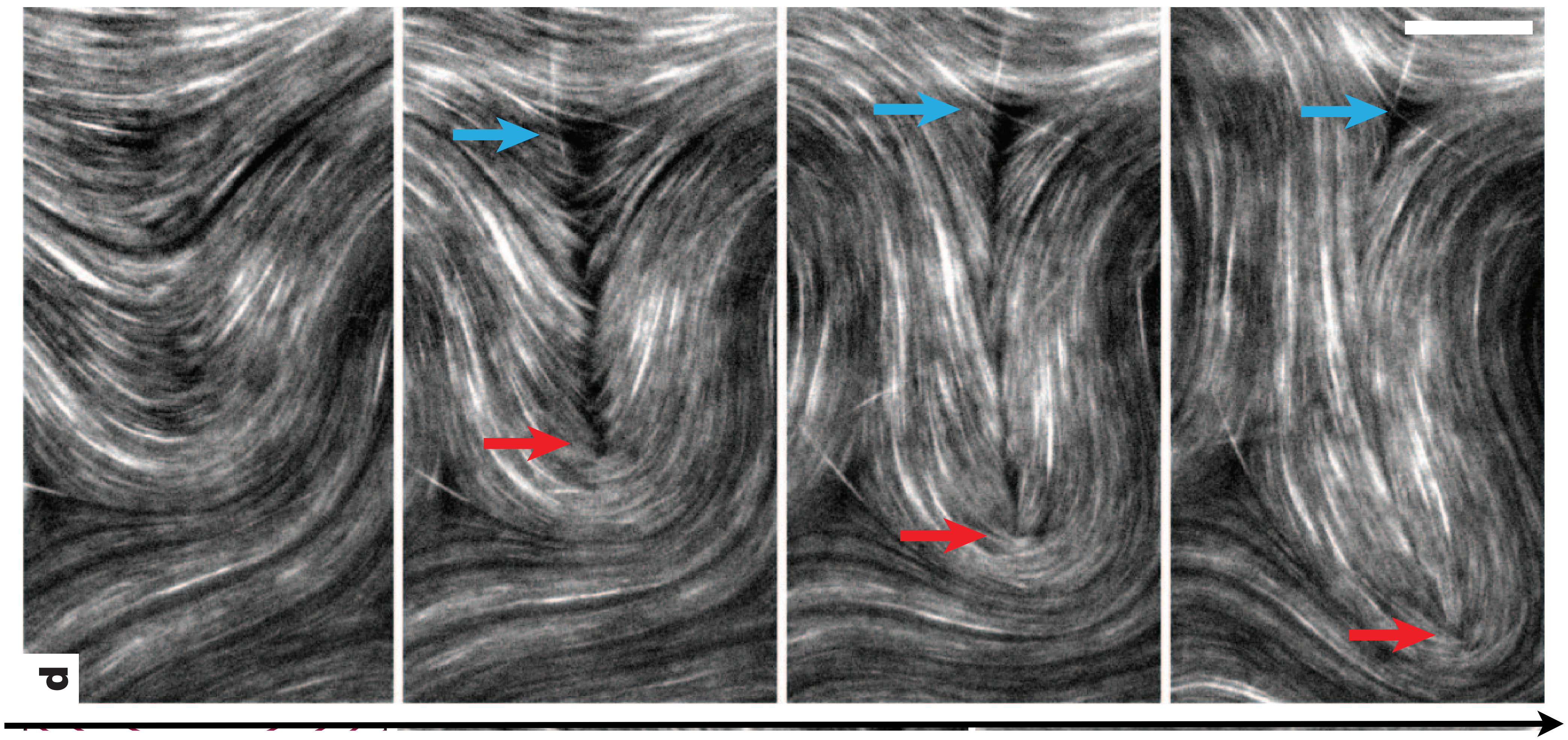

Dogic Lab Brandeis, Science 2012

dunkel@math.mit.edu

This lecture course

- generic PDE models
  - Swift-Hohenberg type higher-order PDEs
  - Reaction-Diffusion (RD) models
- linear stability analysis

arxiv: 1208.4464

Symmetry breaking near boundaries

Broken reflection-symmetry at surfaces

Gibbons (1980) JCB

Sea urchin sperm

in bulk (dilute)

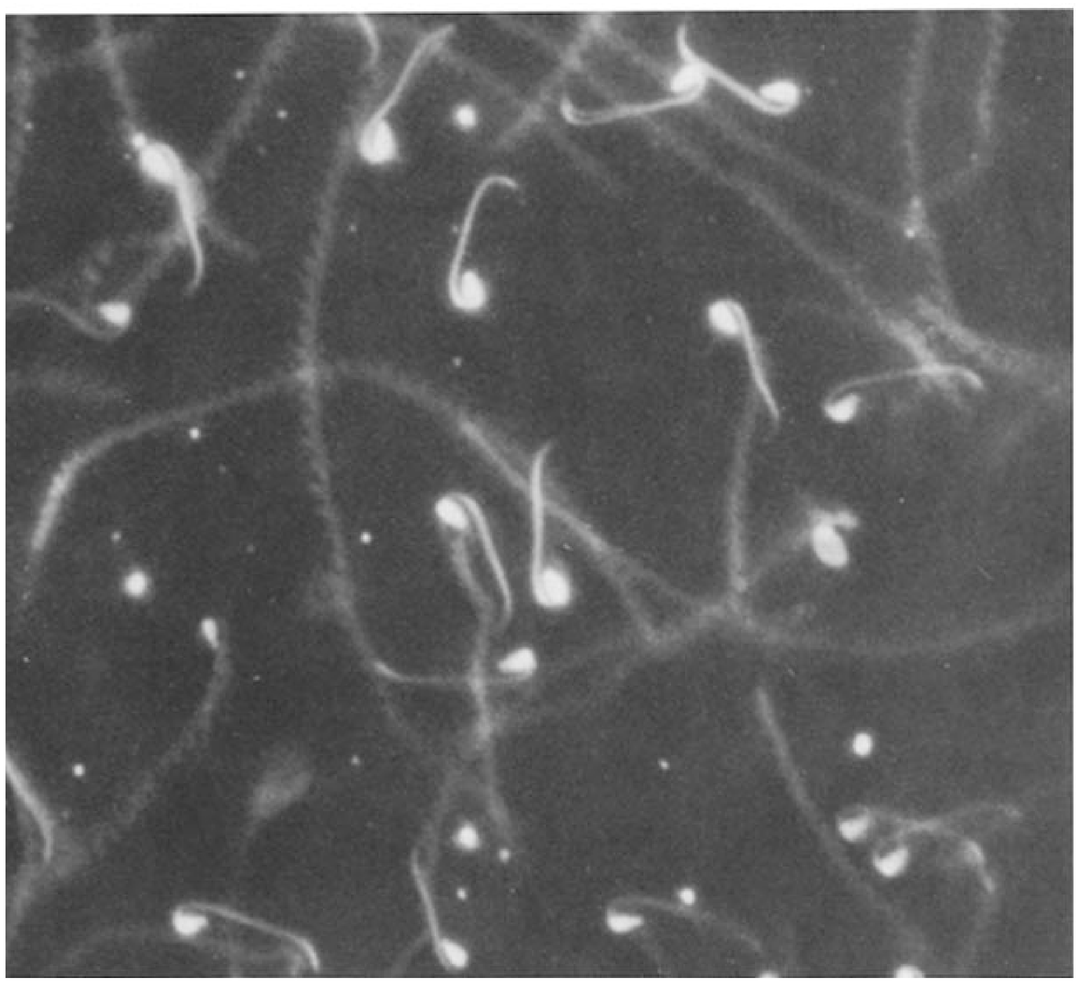

near surface (dilute)

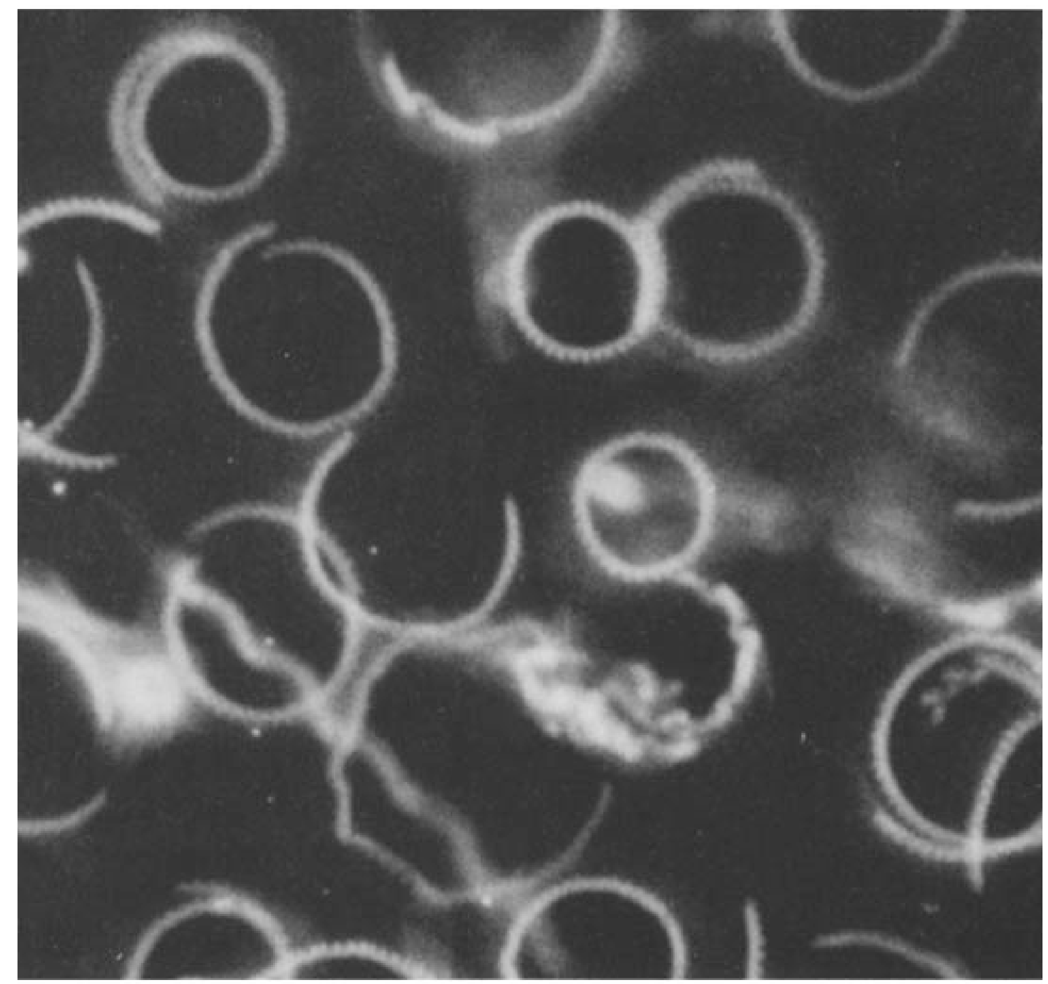

similar for bacteria (E. coli): Di Luzio et al (2005) Nature

2d Swift-Hohenberg model

arxiv: 1208.4464

$$\partial_t \psi = -U'(\psi) + \gamma_0 \nabla^2 \psi - \gamma_2 (\nabla^2)^2 \psi$$

$$U(\psi) = \frac{a}{2}\psi^2 + \cancel{\frac{b}{3}\psi^3} + \frac{c}{4}\psi^4$$

$$\psi(t, \boldsymbol{x}) = \nabla \times \boldsymbol{v}$$

reflection-symmetry

$$b = 0$$

$$\psi \mapsto -\psi$$

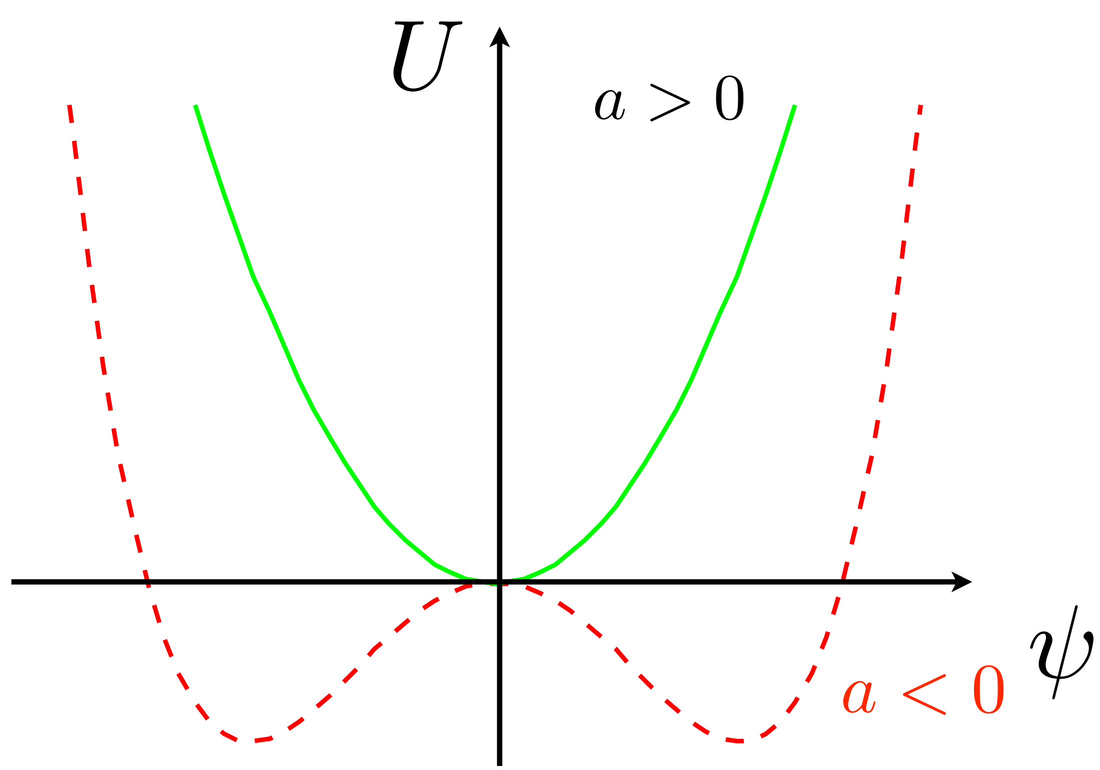

arxiv: 1208.4464

2d Swift-Hohenberg model

$$\partial_t \psi = -U'(\psi) + \gamma_0 \nabla^2 \psi - \gamma_2 (\nabla^2)^2 \psi$$

$$U(\psi) = \frac{a}{2}\psi^2 + \cancel{\frac{b}{3}\psi^3} + \frac{c}{4}\psi^4$$

$$\psi(t, \boldsymbol{x}) = \nabla \times \boldsymbol{v}$$

reflection-symmetry

$$b = 0$$

$$\psi \mapsto -\psi$$

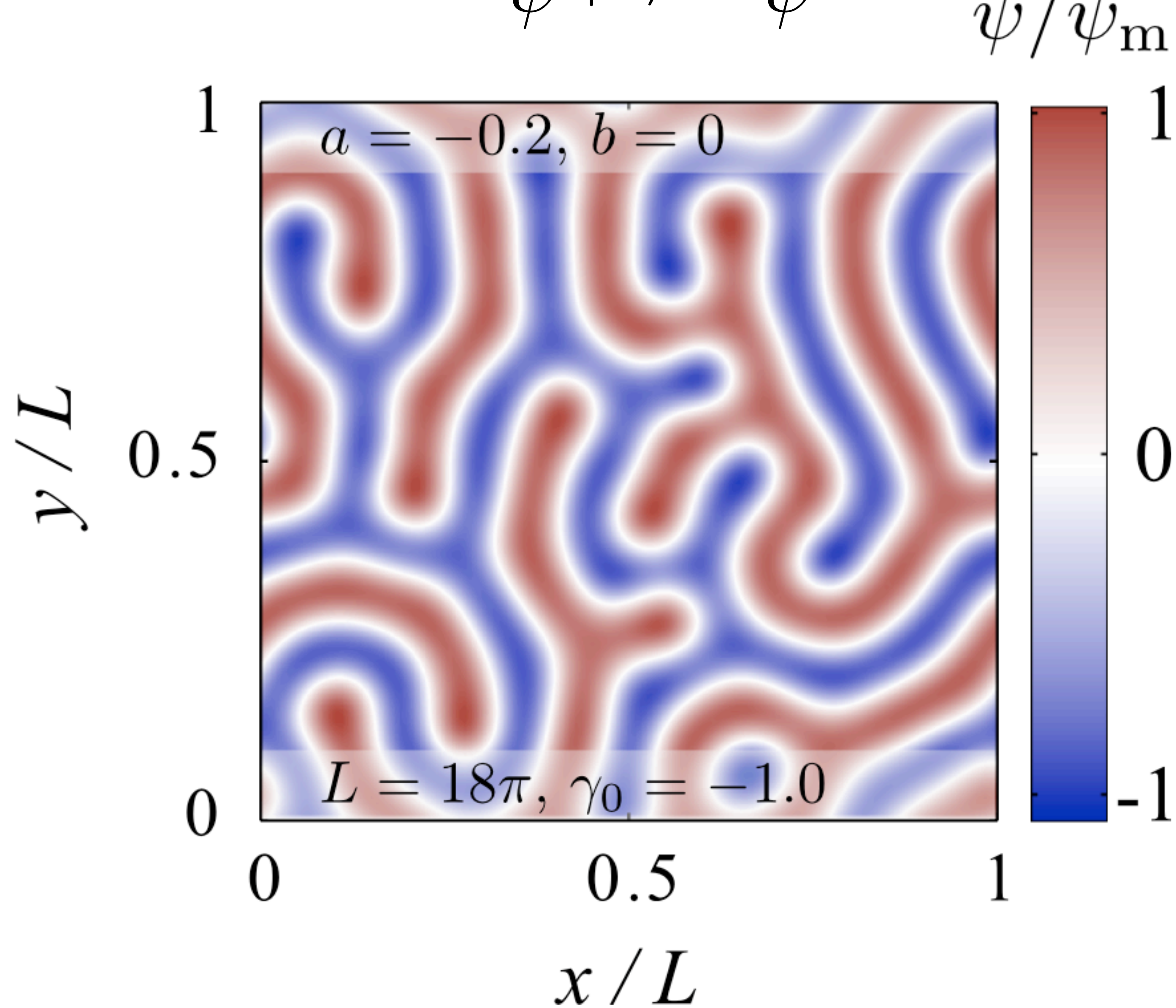

2d Swift-Hohenberg model

arxiv: 1208.4464

$$\partial_t \psi = -U'(\psi) + \gamma_0 \nabla^2 \psi - \gamma_2 (\nabla^2)^2 \psi$$

$$U(\psi) = \frac{a}{2}\psi^2 + \frac{b}{3}\psi^3 + \frac{c}{4}\psi^4$$

$$\psi(t, \boldsymbol{x}) = \nabla \times \boldsymbol{v}$$

broken
reflection-symmetry

$$b \neq 0$$

$$\psi \not\mapsto -\psi$$

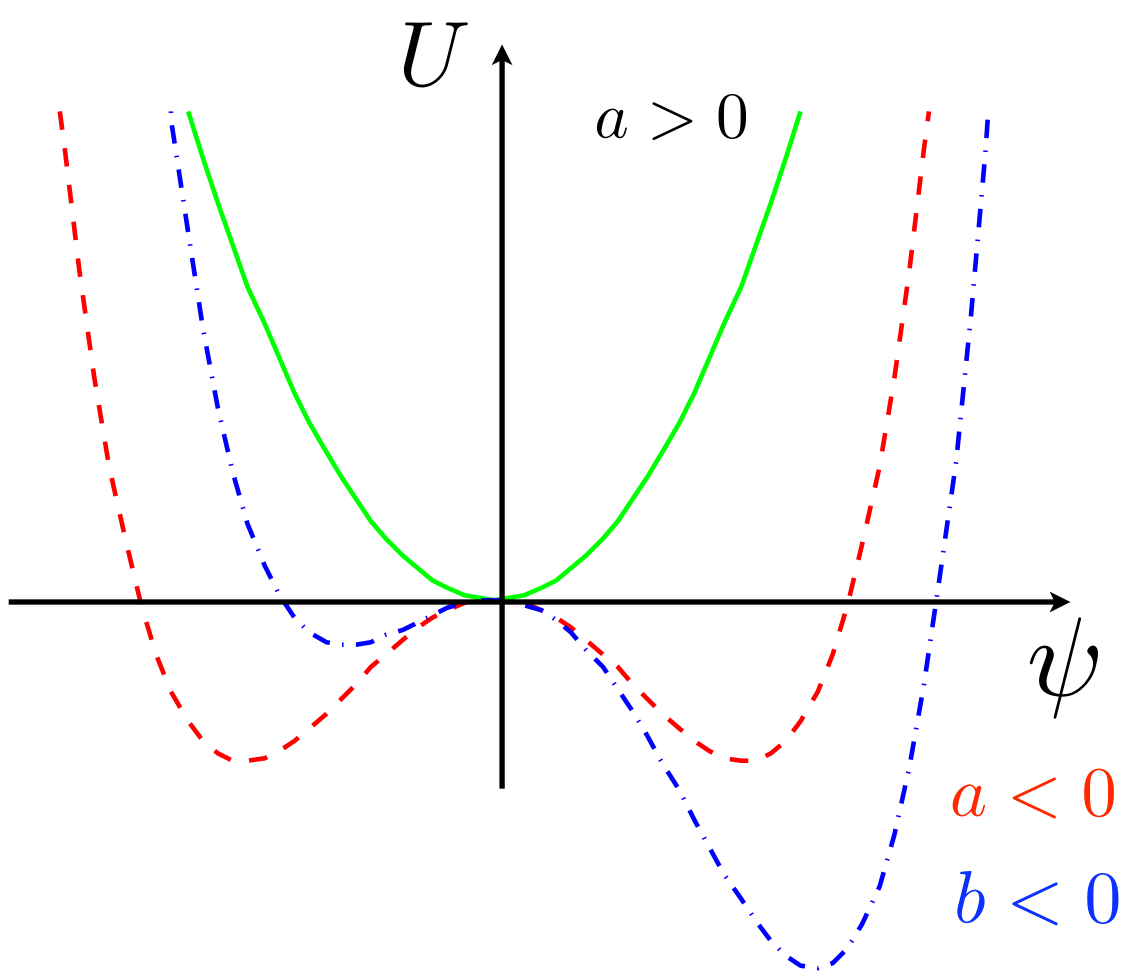

2d Swift-Hohenberg model

arxiv: 1208.4464

$$\partial_t \psi = -U'(\psi) + \gamma_0 \nabla^2 \psi - \gamma_2 (\nabla^2)^2 \psi$$

$$U(\psi) = \frac{a}{2}\psi^2 + \frac{b}{3}\psi^3 + \frac{c}{4}\psi^4$$

$$\psi(t, \boldsymbol{x}) = \nabla \times \boldsymbol{v}$$

broken reflection-symmetry

$$b \neq 0$$

$$\psi \not\mapsto -\psi$$

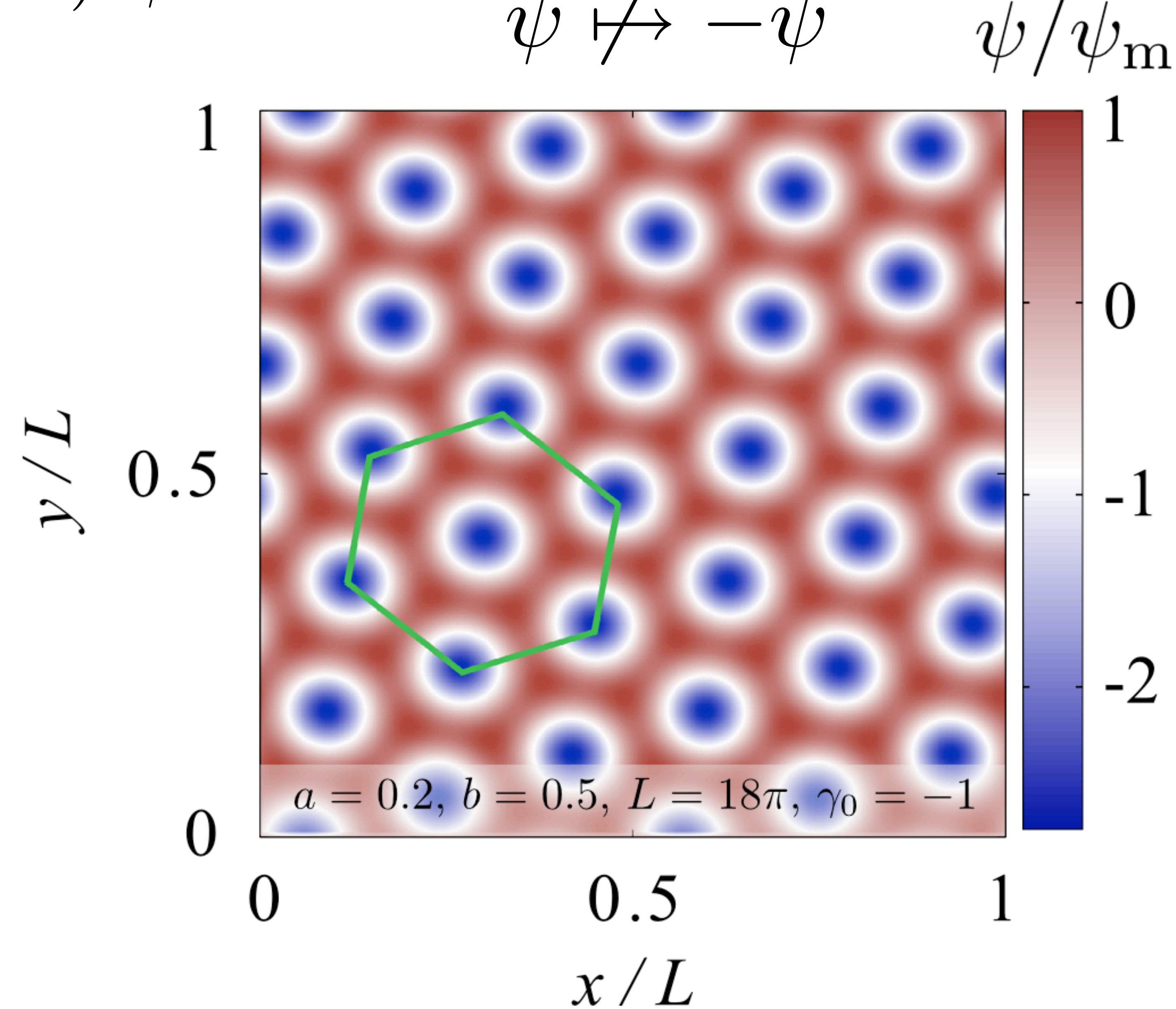

2d Swift-Hohenberg model

arxiv: 1208.4464

Sea urchin sperm cells
near surface
(high concentration)

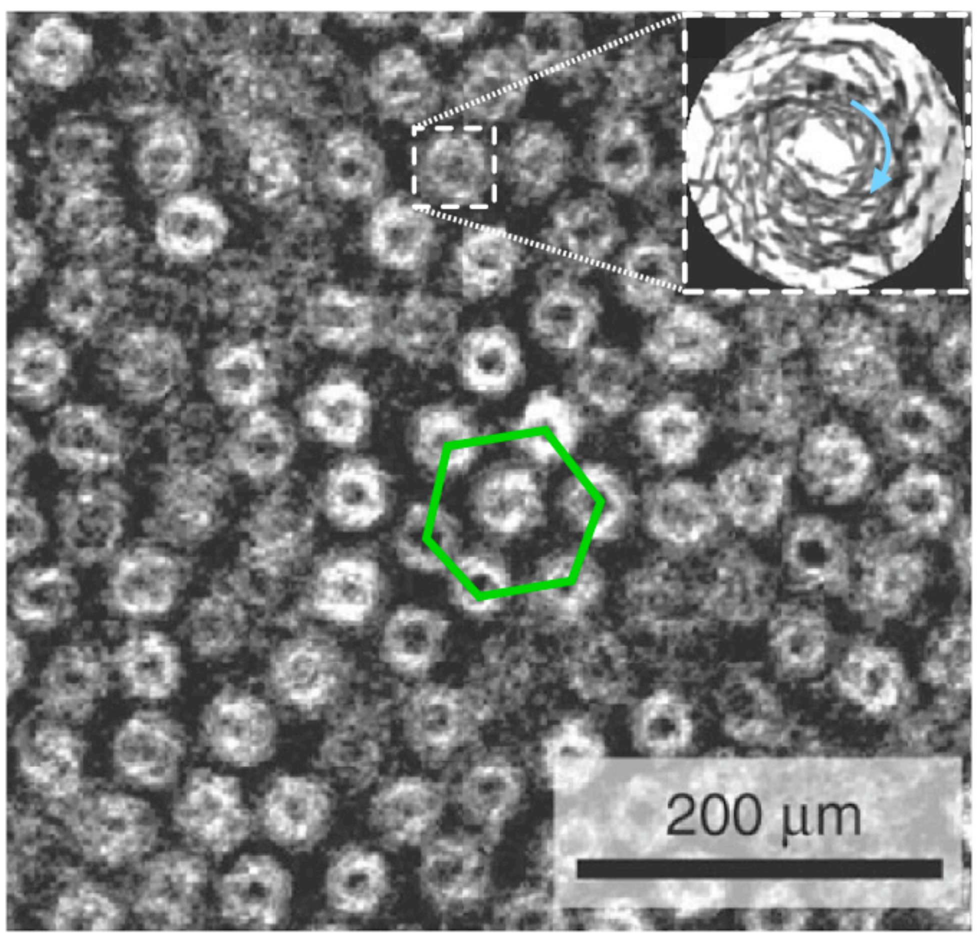

Riedel et al (2007) Science

broken
reflection-symmetry

$$b \neq 0$$

$$\psi \not\mapsto -\psi$$

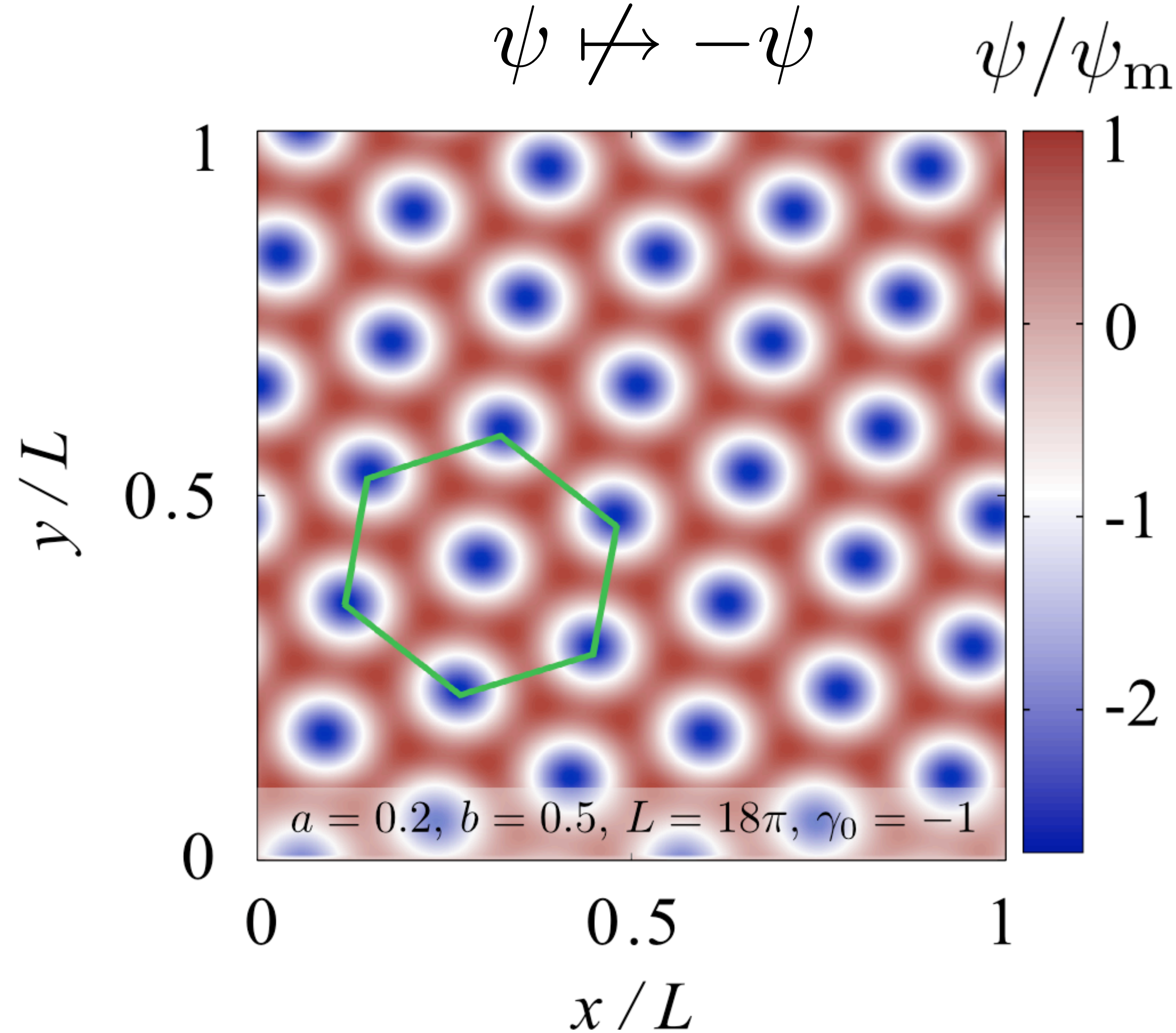

Turing model

$$\frac{\partial u}{\partial t} = F(u,v) - d_u v + D_u \Delta u$$

$$\frac{\partial v}{\partial t} = G(u,v) - d_v v + D_v \Delta v$$

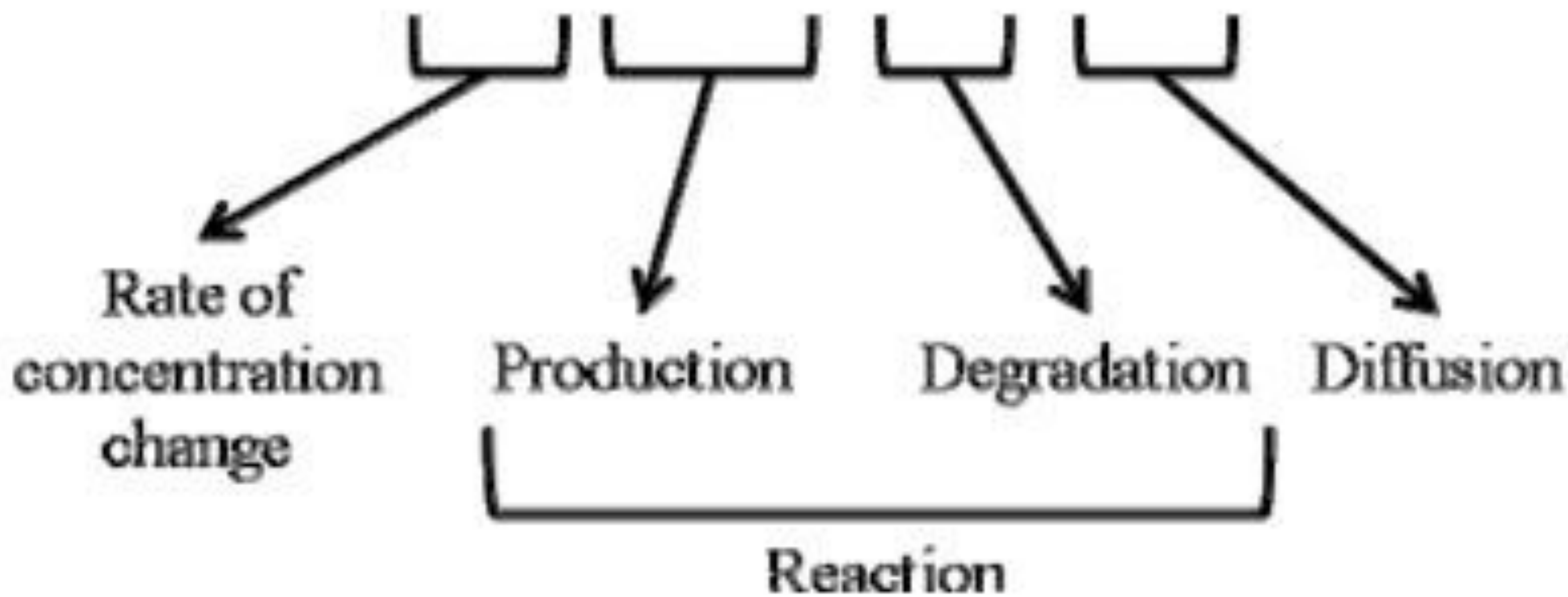

A. M. Turing. **[The chemical basis of morphogenesis.]** *Phil. Trans. Royal Soc. London. B* **327**, 37–72 (1952)

Turing model

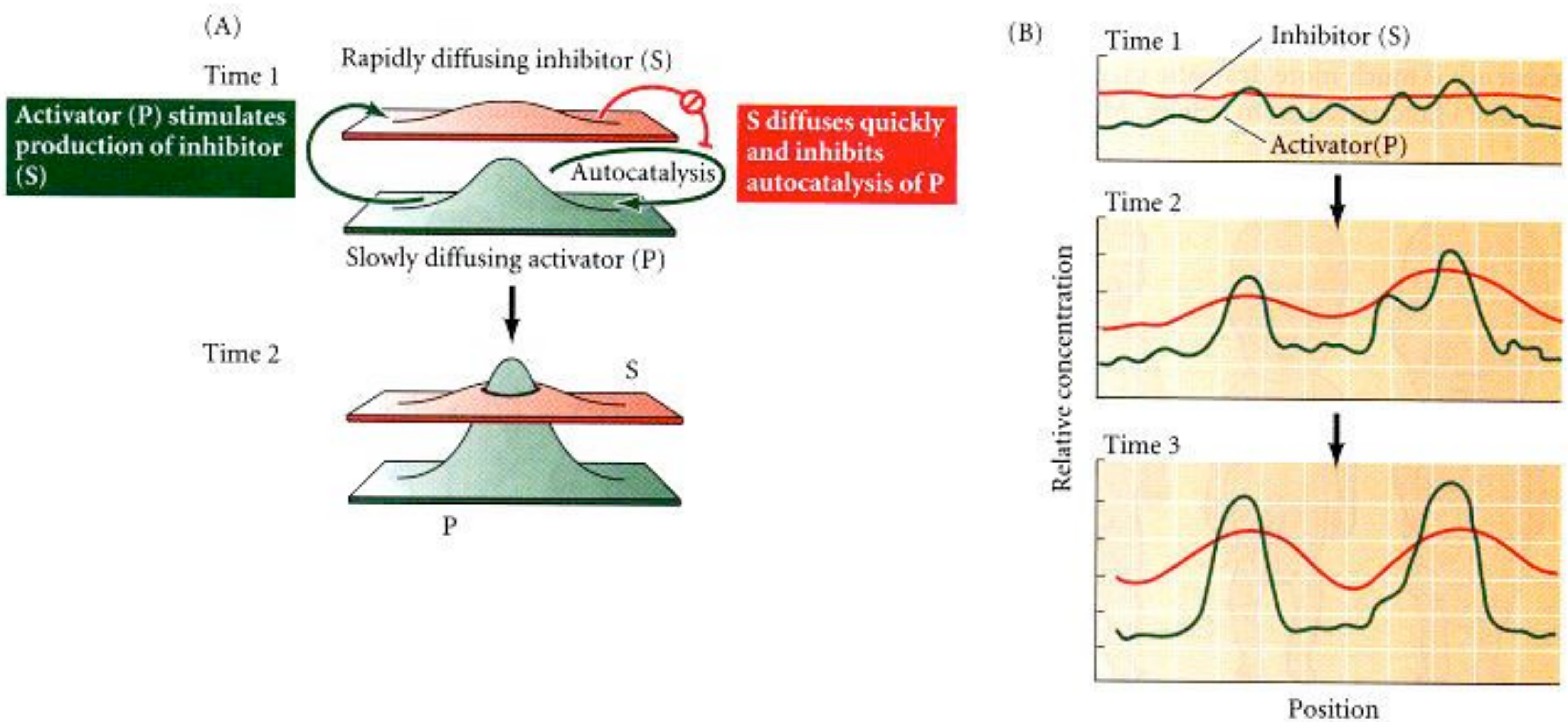

Turing pattern

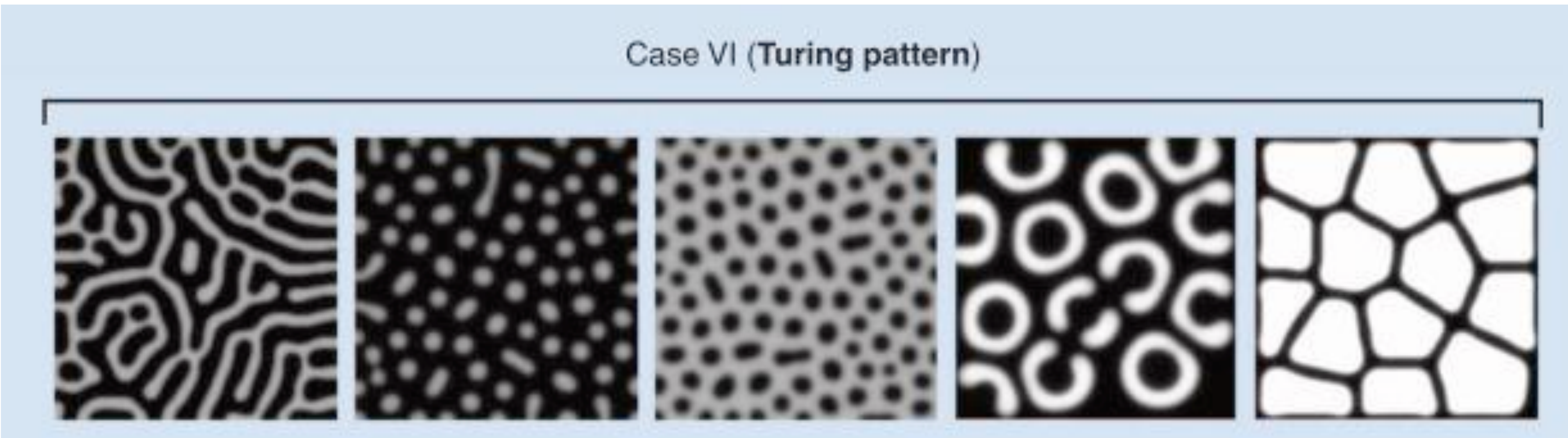

Kondo S, & Miura T (2010). Reaction-diffusion model as a framework for understanding biological pattern formation. *Science, 329* (5999), 1616-20

The matching of zebrafish stripe formation and a Turing model

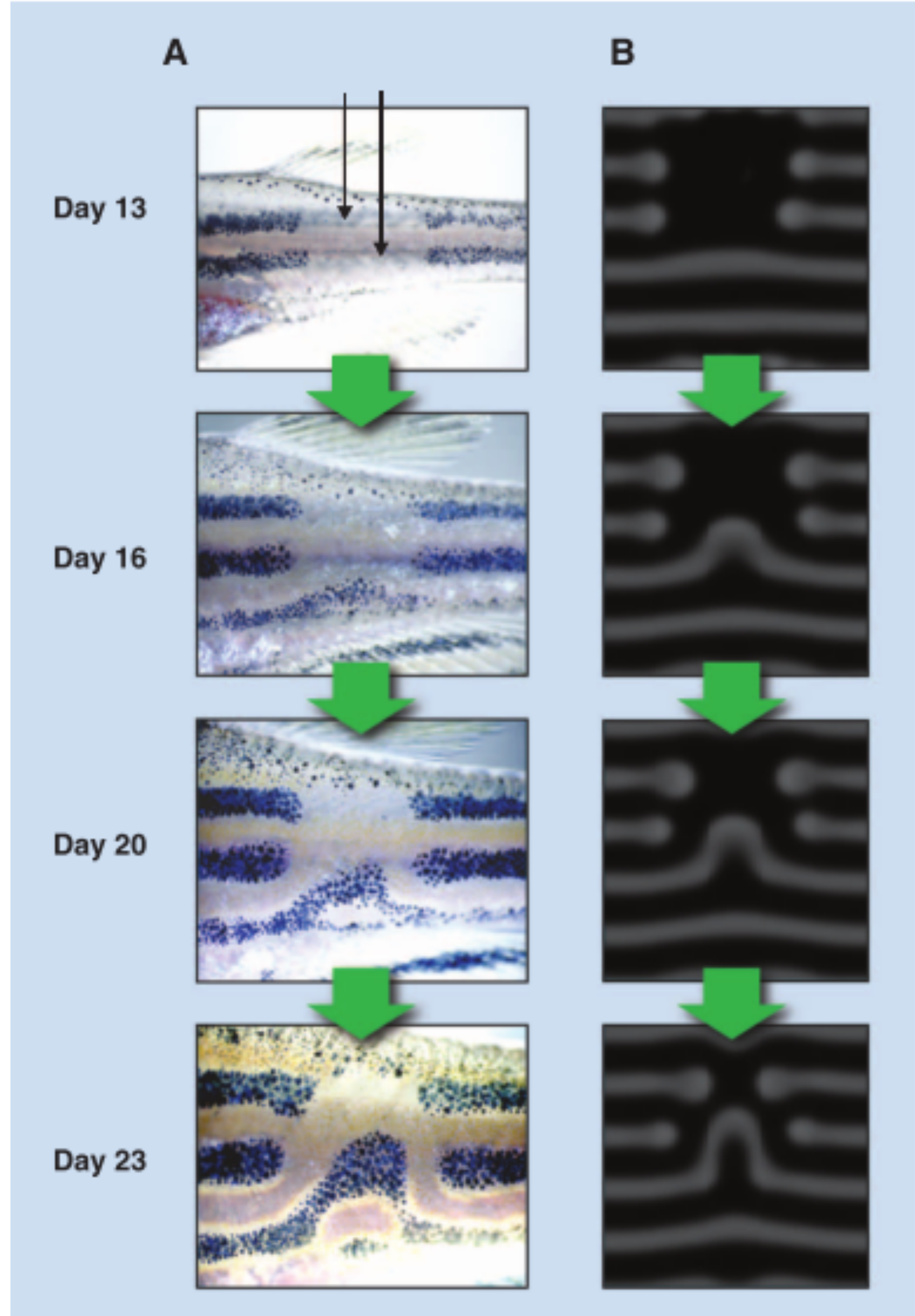

Kondo S, & Miura T (2010). Reaction-diffusion model as a framework for understanding biological pattern formation. *Science, 329* (5999), 1616-20

dunkel@math.mit.edu

Chapter 4

Pattern formation

4.1 Warm-up

Consider a scalar density $\rho(t,x)$, governed by the simple diffusion equation

$$\rho_t = D\rho_{xx} \tag{4.1a}$$

with reflecting boundary conditions on $[0, L]$,

$$\rho_x(t,0) = \rho_x(t,L) = 0. \tag{4.1b}$$

This dynamics defined by Eqs. (4.1) conserves the total 'mass'

$$M(t) = \int_0^L dx\; \rho(t,x) \equiv M_0, \tag{4.2}$$

and a spatially homogeneous stationary solution is given by

$$\rho_0 = M_0/L. \tag{4.3}$$

To evaluate its stability, we can consider wave-like perturbations

$$\rho(t,x) = \rho_0 + \delta\rho(t,x)\ , \qquad \delta\rho = \epsilon\, e^{\sigma t - ikx}. \tag{4.4}$$

Inserting this perturbation ansatz into (4.1) gives

$$\sigma(k) = -Dk^2 \geq 0 \tag{4.5}$$

signaling that ρ_0 is a stable solution, because all modes with $|k| > 0$ become exponentially damped.

dunkel@math.mit.edu

4.2 Swift-Hohenberg model

As a simple generalization of (4.1), we consider the simplest isotropic fourth-order model [DHBG13] for a non-conserved scalar or pseudo-scalar order-parameter $\psi(t, \mathbf{x})$, given by

$$\partial_t \psi = F(\psi) + \gamma_0 \Delta \psi - \gamma_2 \Delta^2 \psi, \tag{4.6}$$

where $\partial_t = \partial/\partial t$ denotes the time derivative, and $\triangle = \nabla^2$ is the d-dimensional Laplacian. The force F is derived from a Landau-potental $U(\psi)$

$$F = -\frac{\partial U}{\partial \psi}, \qquad U(\psi) = \frac{a}{2}\psi^2 + \frac{b}{3}\psi^3 + \frac{c}{4}\psi^4, \tag{4.7}$$

where $c > 0$ to ensure stability.

---

[1]To see this, consider a functional $\mathcal{F}$ that depends on some real-valued fields $\phi_k(x_1, \ldots, x_d), k = 1, \ldots, N$, and their first and second derivatives, and can be written as

$$\mathcal{F}[\phi] = \int d^d x \, F(\phi_k, \partial_i \phi_k, \partial_{ij} \phi_k), \tag{4.8}$$

where $\phi = (\phi_k)$ and $\partial_i = \partial/\partial x_i$, $\partial_{ij} = \partial^2/\partial x_i \partial x_j$. Assuming $F(\eta_k, \xi_{ik}, \zeta_{ijk})$ is a quadratic polynomial in ξ_{ik} and ζ_{ijk}, the functional derivative of $\mathcal{F}$ with respect to ϕ_k is given by

$$\frac{\delta \mathcal{F}}{\delta \phi_k} = \frac{\partial F}{\partial \phi_k} - \partial_i \frac{\partial F}{\partial(\partial_i \phi_k)} + \partial_{ij} \frac{\partial F}{\partial(\partial_{ij} \phi_k)}, \tag{4.9}$$

with a summation convention for identical indices $i, j = 1, \ldots, d$.

4.2 Swift-Hohenberg model

As a simple generalization of (4.1), we consider the simplest isotropic fourth-order model [DHBG13] for a non-conserved scalar or pseudo-scalar order-parameter $\psi(t, \mathbf{x})$, given by

$$\partial_t \psi = F(\psi) + \gamma_0 \Delta\psi - \gamma_2 \Delta^2 \psi, \tag{4.6}$$

where $\partial_t = \partial/\partial t$ denotes the time derivative, and $\triangle = \nabla^2$ is the d-dimensional Laplacian. The force F is derived from a Landau-potental $U(\psi)$

$$F = -\frac{\partial U}{\partial \psi}, \qquad U(\psi) = \frac{a}{2}\psi^2 + \frac{b}{3}\psi^3 + \frac{c}{4}\psi^4, \tag{4.7}$$

where $c > 0$ to ensure stability.

The derivative terms on the rhs. of (4.6) can also be obtained by variational methods from a suitably defined energy functional,[1]

$$\partial_t \psi = -\frac{\delta \mathcal{F}}{\delta \psi}, \tag{4.10}$$

where

$$\mathcal{F}[\psi] = \int d^d x \, \left[\frac{1}{2}\gamma_0(\nabla\psi)\cdot(\nabla\psi) + \frac{1}{2}\gamma_2(\triangle\psi)(\triangle\psi) + U(\psi)\right]. \tag{4.11}$$

dunkel@math.mit.edu

Note on ‘mass’ conservation

[2]For completeness, one should also note that in the case of a conserved order-parameter field ϱ the field equations would either have to take the current-form $\partial_t \varrho = -\nabla \cdot \mathbf{J}(\varrho)$ or, alternatively, one can also implement conservation laws globally by means of Lagrange multipliers. To illustrate this briefly, let us consider a system that is confined to a finite spatial domain $\Omega \subset \mathbb{R}^d$ of volume

$$|\Omega| = \int_\Omega d^d x \tag{4.12}$$

and described by a density ϱ that is subject to a global ‘mass’ constraint

$$M = \int_\Omega d^d x \, \varrho = const.$$

Assuming the dynamics of ϱ is governed by an equation similar to (4.6), the Lagrange-multiplier approach yields the non-local equation

$$\begin{aligned}
\partial_t \varrho &= F(\varrho) + \gamma_0 \Delta \varrho - \gamma_2 \Delta^2 \varrho - \lambda_1, \\
\lambda_1 &= \frac{1}{|\Omega|} \int_\Omega d^d x \, \left[F(\varrho) + \gamma_0 \Delta \varrho - \gamma_2 \Delta^2 \varrho \right].
\end{aligned}$$

dunkel@math.mit.edu

$$\partial_t \psi = F(\psi) + \gamma_0 \Delta\psi - \gamma_2 \Delta^2 \psi, \qquad F = -\frac{\partial U}{\partial \psi}, \qquad U(\psi) = \frac{a}{2}\psi^2 + \frac{b}{3}\psi^3 + \frac{c}{4}\psi^4$$

4.2.1 Linear stability analysis

The fixed points of (4.6) are determined by the zeros of the force $F(\psi)$, corresponding to the minima of the potential U, yielding

$$\psi_0 = 0 \tag{4.13a}$$

and

$$\psi_\pm = -\frac{b}{2c} \pm \sqrt{\frac{b^2}{4c^2} - \frac{a}{c}}, \qquad \text{if} \quad b^2 > 4ac. \tag{4.13b}$$

Linearization of (4.6) near ψ_0 for small perturbations

$$\delta\psi = \epsilon_0 \exp(\sigma_0 t - i\mathbf{k}\cdot\mathbf{x}) \tag{4.14}$$

gives

$$\sigma_0(\mathbf{k}) = -(a + \gamma_0|\mathbf{k}|^2 + \gamma_2|\mathbf{k}|^4). \tag{4.15}$$

Similarly, one finds for

$$\psi = \psi_\pm + \epsilon_\pm \exp(\sigma_\pm t - i\mathbf{k}\cdot\mathbf{x}) \tag{4.16}$$

the dispersion relation

$$\sigma_\pm(\mathbf{k}) = -\left[-(2a + b\psi_\pm) + \gamma_0|\mathbf{k}|^2 + \gamma_2|\mathbf{k}|^4\right]. \tag{4.17}$$

$\boxed{k\text{-modes with } \sigma > 0 \text{ are unstable}}$

4.3 Vector model for an incompressible active fluid

4.3.1 Model equations

Postulating incompressibility, which is a good approximation for sufficiently dense suspensions [WDH+12],[5]

$$\nabla \cdot \mathbf{v} = \partial_i v_i = 0, \tag{4.18}$$

we assume that the dynamics of the bacterial mean velocity-field $\mathbf{v}$ is governed by the generalized Navier-Stokes equation

$$(\partial_t + \mathbf{v} \cdot \nabla)\mathbf{v} = -\nabla p - (A + C|\mathbf{v}|^2)\mathbf{v} + \nabla \cdot \mathbf{E}. \tag{4.19}$$

Landau velocity potential [Ram10, TTR05, TT98]

$$U(\mathbf{v}) = \frac{A}{2}|\mathbf{v}|^2 + \frac{C}{4}|\mathbf{v}|^4. \tag{4.20}$$

$$E_{ij} = \Gamma_0(\partial_i v_j + \partial_j v_i) - \Gamma_2 \triangle \left(\partial_i v_j + \partial_j v_i\right) + S\, q_{ij},$$

$$q_{ij} = v_i v_j - \frac{\delta_{ij}}{d}|\mathbf{v}|^2$$

4.3 Vector model for an incompressible active fluid

4.3.1 Model equations

Postulating incompressibility, which is a good approximation for sufficiently dense suspensions [WDH+12],[5]

$$\nabla \cdot \mathbf{v} = \partial_i v_i = 0, \tag{4.18}$$

we assume that the dynamics of the bacterial mean velocity-field $\mathbf{v}$ is governed by the generalized Navier-Stokes equation

$$(\partial_t + \mathbf{v} \cdot \nabla)\mathbf{v} = -\nabla p - (A + C|\mathbf{v}|^2)\mathbf{v} + \nabla \cdot \mathbf{E}. \tag{4.19}$$

Landau velocity potential [Ram10, TTR05, TT98]

$$U(\mathbf{v}) = \frac{A}{2}|\mathbf{v}|^2 + \frac{C}{4}|\mathbf{v}|^4. \tag{4.20}$$

$$\lambda_0 = 1 - S, \qquad \lambda_1 = -S/d, \tag{4.23}$$

we obtain

$$(\partial_t + \lambda_0 \mathbf{v} \cdot \nabla)\mathbf{v} = -\nabla p + \lambda_1 \nabla \mathbf{v}^2 - (A + C|\mathbf{v}|^2)\mathbf{v} + \Gamma_0 \triangle \mathbf{v} - \Gamma_2 \triangle^2 \mathbf{v}. \tag{4.24}$$

$$\nabla \cdot \mathbf{v} = \partial_i v_i = 0, \qquad (\partial_t + \lambda_0 \mathbf{v} \cdot \nabla)\mathbf{v} = -\nabla p + \lambda_1 \nabla \mathbf{v}^2 - (A + C|\mathbf{v}|^2)\mathbf{v} + \Gamma_0 \triangle \mathbf{v} - \Gamma_2 \triangle^2 \mathbf{v}.$$

4.3.2 Linear stability analysis

To support the qualitative statements in the preceding paragraph, we now perform a stability analysis for the 2D case, assuming $\Gamma_0 < 0$ and $C > 0$, $\Gamma_2 > 0$.

$$\text{disordered isotropic state } (\mathbf{v}, p) = (\mathbf{0}, p_0)$$

Linearizing Equations (4.18) and (4.24) for small velocity and pressure perturbations around the isotropic state, $\mathbf{v} = \epsilon$ and $p = p_0 + \eta$ with $|\eta| \ll |p_0|$, and considering perturbations of the form

$$(\eta, \epsilon) = (\hat{\eta}, \hat{\epsilon}) \exp(\sigma_0 t - i\mathbf{k} \cdot \mathbf{x}), \tag{4.25}$$

we find

$$0 = \mathbf{k} \cdot \hat{\epsilon}, \tag{4.26}$$

$$\sigma_0 \hat{\epsilon} = i\hat{\eta}\mathbf{k} - (A + \Gamma_0 |\mathbf{k}|^2 + \Gamma_2 |\mathbf{k}|^4)\hat{\epsilon}. \tag{4.27}$$

Multiplying the second equation by $\mathbf{k}$ and using the incompressibility condition implies that $\hat{\eta} = 0$ and, therefore,

$$\sigma_0(\mathbf{k}) = -\left(A + \Gamma_0 |\mathbf{k}|^2 + \Gamma_2 |\mathbf{k}|^4\right). \tag{4.28}$$

Assuming $\Gamma_0 < 0$ and $\Gamma_2 > 0$, and provided that $4A < |\Gamma_0|^2/\Gamma_2$, we find an unstable band of modes with $\sigma_0(\mathbf{k}) > 0$ for $k_-^2 < |\mathbf{k}|^2 < k_+^2$, where

$$k_\pm^2 = \frac{|\Gamma_0|}{\Gamma_2} \left(\frac{1}{2} \pm \sqrt{\frac{1}{4} - \frac{A\Gamma_2}{|\Gamma_0|^2}} \right). \tag{4.29}$$

For $A < 0$ the isotropic state is generally unstable with respect to long-wavelength (i.e., small-$|\mathbf{k}|$) perturbations.

$$\nabla \cdot \mathbf{v} = \partial_i v_i = 0, \qquad (\partial_t + \lambda_0 \mathbf{v} \cdot \nabla)\mathbf{v} = -\nabla p + \lambda_1 \nabla \mathbf{v}^2 - (A + C|\mathbf{v}|^2)\mathbf{v} + \Gamma_0 \triangle \mathbf{v} - \Gamma_2 \triangle^2 \mathbf{v}.$$

4.3.2 Linear stability analysis

To support the qualitative statements in the preceding paragraph, we now perform a stability analysis for the 2D case, assuming $\Gamma_0 < 0$ and $C > 0$, $\Gamma_2 > 0$.

manifold of globally ordered polar states $(\mathbf{v}, p) = (\mathbf{v}_0, p_0)$: $\quad |\mathbf{v}_0| = \sqrt{-A/C} =: v_0$.

We next perform a similar analysis for the polar state $(\mathbf{v}_0, p_0)$, which is energetically preferred for $A < 0$ and corresponds to all active particles swimming in the same direction ('global order'). In this case, when considering small deviations

$$\mathbf{v} = \mathbf{v}_0 + \epsilon, \qquad p = p_0 + \eta, \tag{4.30}$$

it is useful to distinguish perturbations perpendicular and parallel to $\mathbf{v}_0$, by writing $\epsilon = \epsilon_{||} + \epsilon_\perp$ where $\mathbf{v}_0 \cdot \epsilon_\perp = 0$ and $\mathbf{v}_0 \cdot \epsilon_{||} = v_0 \epsilon_{||}$. Without loss of generality, we may choose $\mathbf{v}_0$ to point along the x-axis, $\mathbf{v}_0 = v_0 \mathbf{e}_x$. Adopting this convention, we have $\epsilon_{||} = (\epsilon_{||}, 0)$ and $\epsilon_\perp = (0, \epsilon_\perp)$, and to leading order

$$|\mathbf{v}|^2 \simeq v_0^2 + 2 v_0 \epsilon_{||}. \tag{4.31}$$

Linearization for exponential perturbations of the form

$$(\eta, \epsilon_{||}, \epsilon_\perp) = (\hat{\eta}, \hat{\epsilon}_{||}, \hat{\epsilon}_\perp) \exp(\sigma t - i\mathbf{k} \cdot \mathbf{x}) \tag{4.32}$$

dunkel@math.mit.edu

$$\nabla \cdot \mathbf{v} = \partial_i v_i = 0, \qquad (\partial_t + \lambda_0 \mathbf{v} \cdot \nabla)\mathbf{v} = -\nabla p + \lambda_1 \nabla \mathbf{v}^2 - (A + C|\mathbf{v}|^2)\mathbf{v} + \Gamma_0 \triangle \mathbf{v} - \Gamma_2 \triangle^2 \mathbf{v}.$$

4.3.2 Linear stability analysis

To support the qualitative statements in the preceding paragraph, we now perform a stability analysis for the 2D case, assuming $\Gamma_0 < 0$ and $C > 0$, $\Gamma_2 > 0$.

manifold of globally ordered polar states $(\mathbf{v}, p) = (\mathbf{v}_0, p_0)$. $\quad |\mathbf{v}_0| = \sqrt{-A/C} =: v_0.$

yields

$$\begin{aligned} 0 &= \mathbf{k} \cdot \hat{\epsilon}, &\text{(4.33a)}\\ \sigma \hat{\epsilon} &= i(\hat{\eta} - 2v_0 \lambda_1 \hat{\epsilon}_{||})\mathbf{k} + \mathbf{M}\hat{\epsilon}, &\text{(4.33b)}\end{aligned}$$

where

$$\mathbf{M} = \begin{pmatrix} 2A & 0 \\ 0 & 0 \end{pmatrix} - (\Gamma_0 |\mathbf{k}|^2 + \Gamma_2 |\mathbf{k}|^4 - i\lambda_0 k_x v_0)\mathbf{I} \tag{4.34}$$

with $\mathbf{I} = (\delta_{ij})$ denoting the identity matrix. Multiplying Equation (4.33b) with $i\mathbf{k}$, and using the incompressibility condition (4.33a), gives

$$\hat{\eta} = 2v_0 \lambda_1 \epsilon_{||} + i \frac{\mathbf{k} \cdot (\mathbf{M}\hat{\epsilon})}{|\mathbf{k}|^2}. \tag{4.35}$$

Inserting this into Equation (4.33b) and defining $\mathbf{M}_\perp = \mathbf{\Pi}(\mathbf{k})\mathbf{M}$, where

$$\Pi_{ij}(\mathbf{k}) = \delta_{ij} - \frac{k_i k_j}{|\mathbf{k}|^2} \tag{4.36}$$

is the orthogonal projector of $\mathbf{k}$, we obtain

$$\sigma \hat{\epsilon} = \mathbf{M}_\perp \hat{\epsilon}. \tag{4.37}$$

dunkel@math.mit.edu

$$\nabla \cdot \mathbf{v} = \partial_i v_i = 0, \qquad (\partial_t + \lambda_0 \mathbf{v} \cdot \nabla)\mathbf{v} = -\nabla p + \lambda_1 \nabla \mathbf{v}^2 - (A + C|\mathbf{v}|^2)\mathbf{v} + \Gamma_0 \triangle \mathbf{v} - \Gamma_2 \triangle^2 \mathbf{v}.$$

4.3.2 Linear stability analysis

To support the qualitative statements in the preceding paragraph, we now perform a stability analysis for the 2D case, assuming $\Gamma_0 < 0$ and $C > 0$, $\Gamma_2 > 0$.

manifold of globally ordered polar states $(\mathbf{v}, p) = (\mathbf{v}_0, p_0)$: $\quad |\mathbf{v}_0| = \sqrt{-A/C} =: v_0$.

yields

$$\begin{aligned} 0 &= \mathbf{k} \cdot \hat{\epsilon}, & (4.33a) \\ \sigma\, \hat{\epsilon} &= i(\hat{\eta} - 2v_0\lambda_1\hat{\epsilon}_{||})\mathbf{k} + \mathbf{M}\hat{\epsilon}, & (4.33b) \end{aligned}$$

where

$$\mathbf{M} = \begin{pmatrix} 2A & 0 \\ 0 & 0 \end{pmatrix} - (\Gamma_0|\mathbf{k}|^2 + \Gamma_2|\mathbf{k}|^4 - i\lambda_0 k_x v_0)\mathbf{I} \tag{4.34}$$

The eigenvalue spectrum of the matrix $\mathbf{M}_\perp$ is given by

$$\sigma(\mathbf{k}) \in \left\{0, i\lambda_0 v_0 k_x - \left(\Gamma_0|\mathbf{k}|^2 + \Gamma_2|\mathbf{k}|^4 - 2A\frac{k_x^2}{|\mathbf{k}|^2}\right)\right\}. \tag{4.38}$$

experiment *vs.* theory

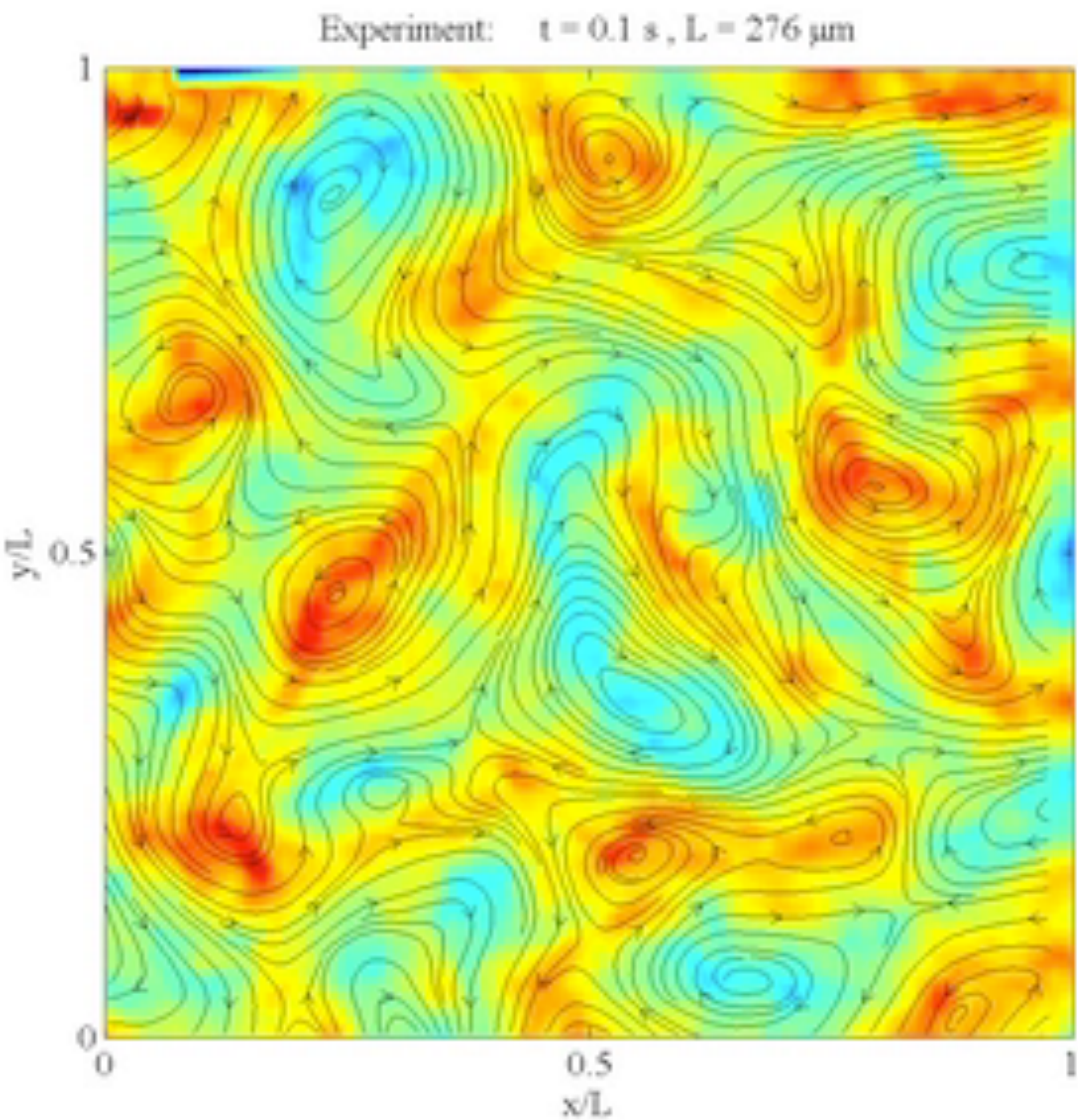

quasi-2D slice

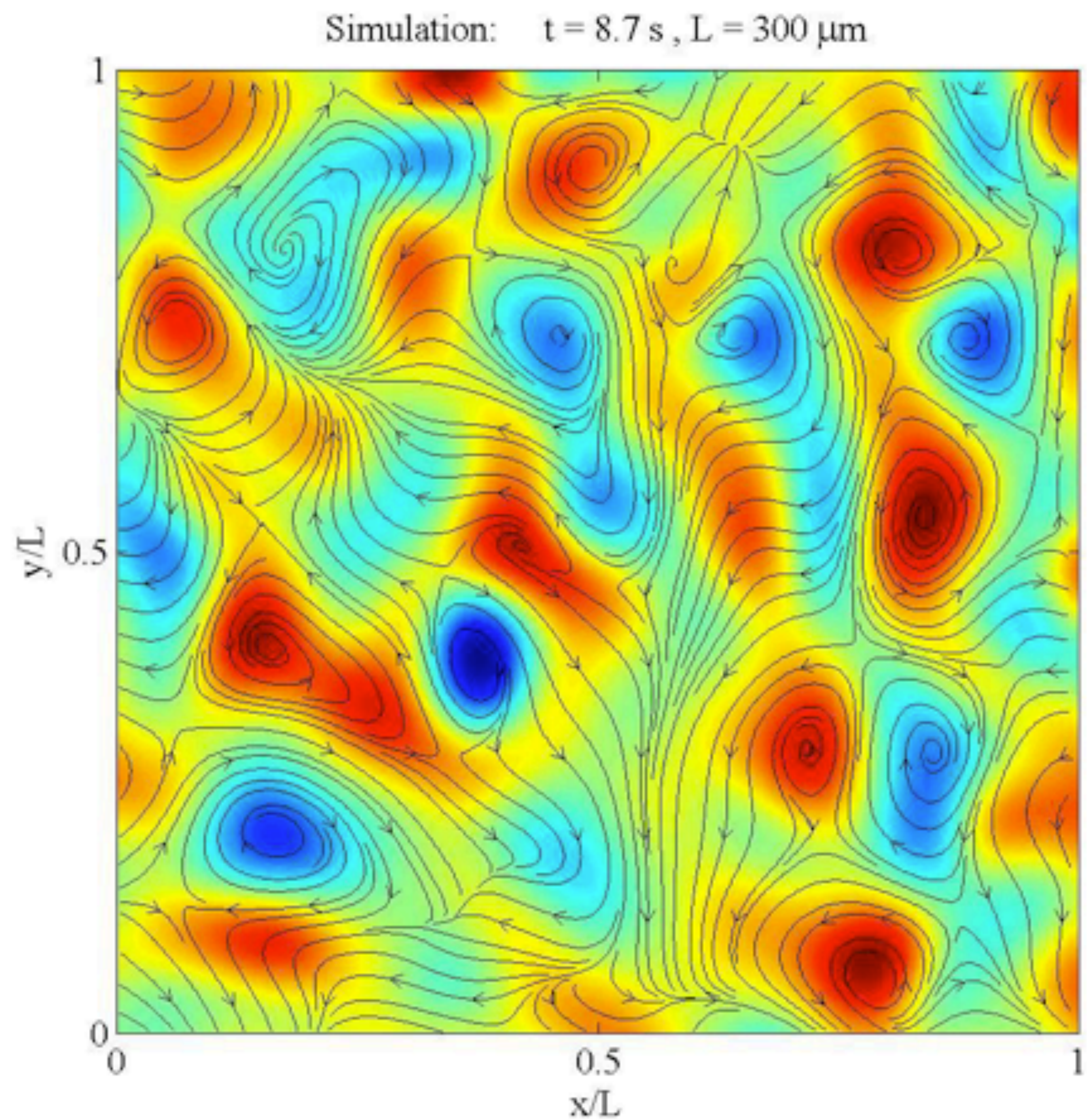

2D slice
from 3D simulation

Dunkel et al PRL 2013

Velocity correlations

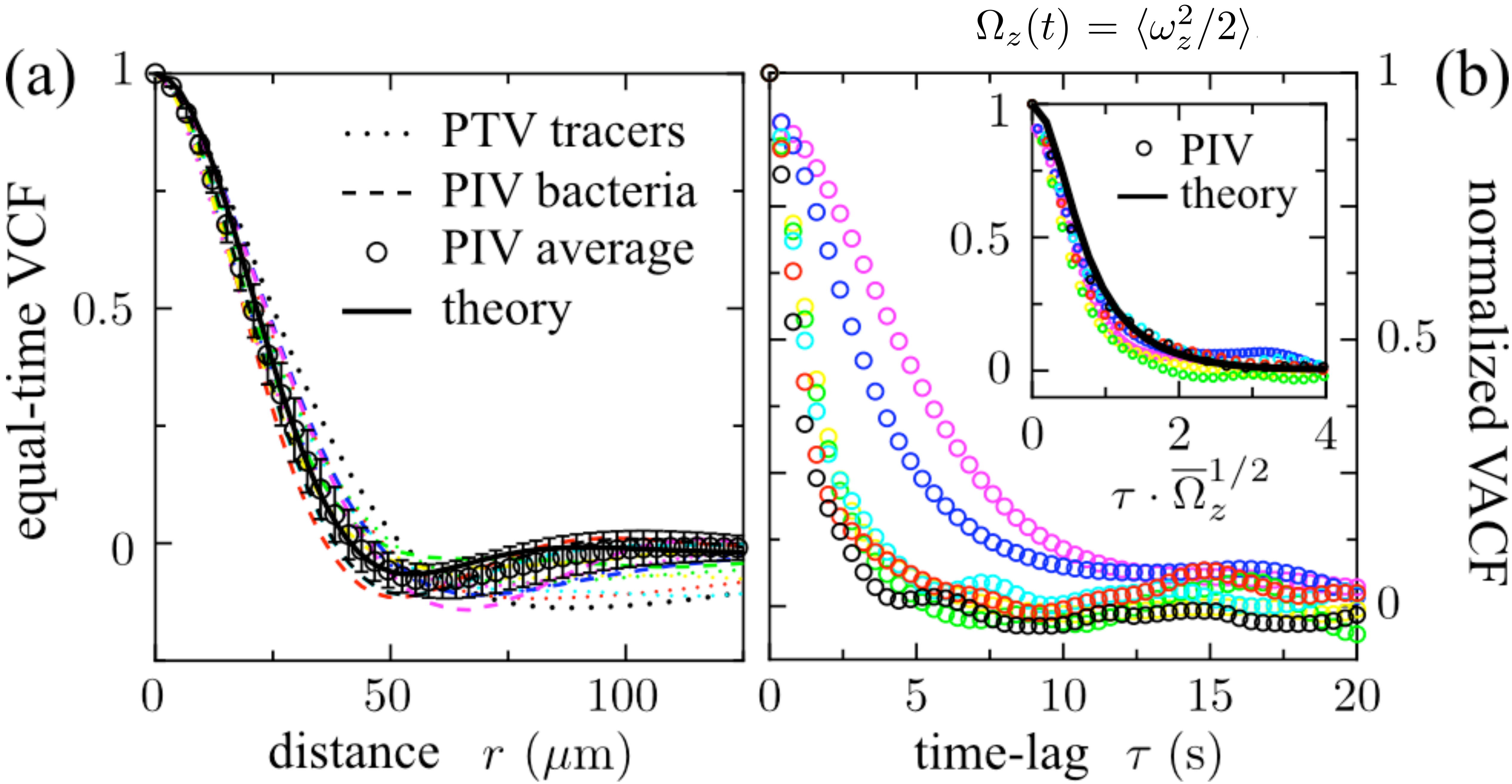

Vortex diameter ~ 70μm

Vortex life time ~ seconds

Dunkel et al PRL 2013

Future goal: predict shear properties

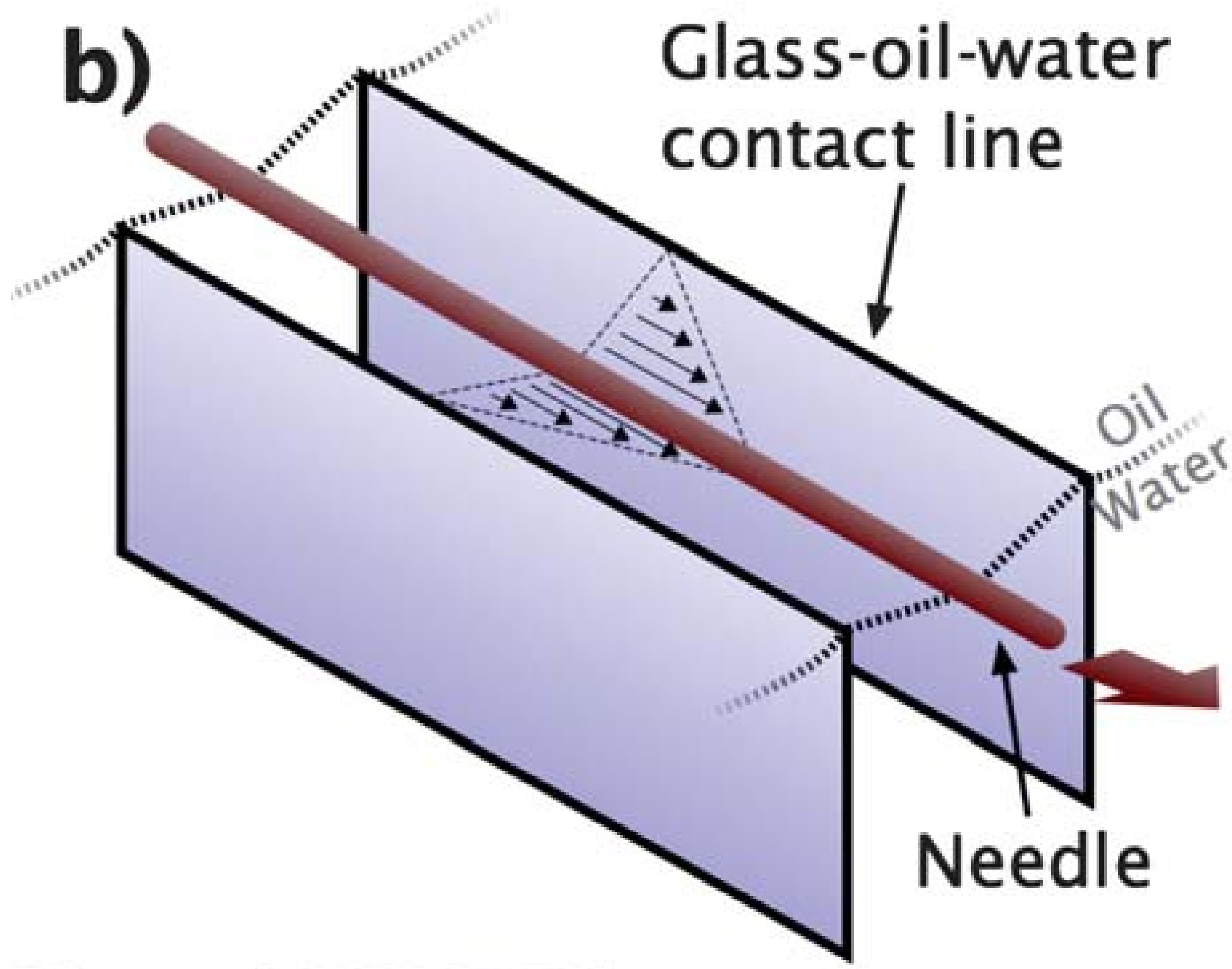

Soft Matter 2013

Arratia lab (UPenn)

Minimal momentum-conserving model

Flow equations

$$
\begin{aligned}
0 &= \nabla \cdot \boldsymbol{v} \\
\partial_t \boldsymbol{v} + (\boldsymbol{v} \cdot \nabla)\boldsymbol{v} &= -\nabla p + \nabla \cdot \boldsymbol{\sigma}
\end{aligned}
$$

with stress tensor

$$
\boldsymbol{\sigma} = [\Gamma_0 - \Gamma_2(\nabla^2) + \Gamma_4(\nabla^2)^2](\nabla^\top \boldsymbol{v} + \nabla \boldsymbol{v}^\top)
$$

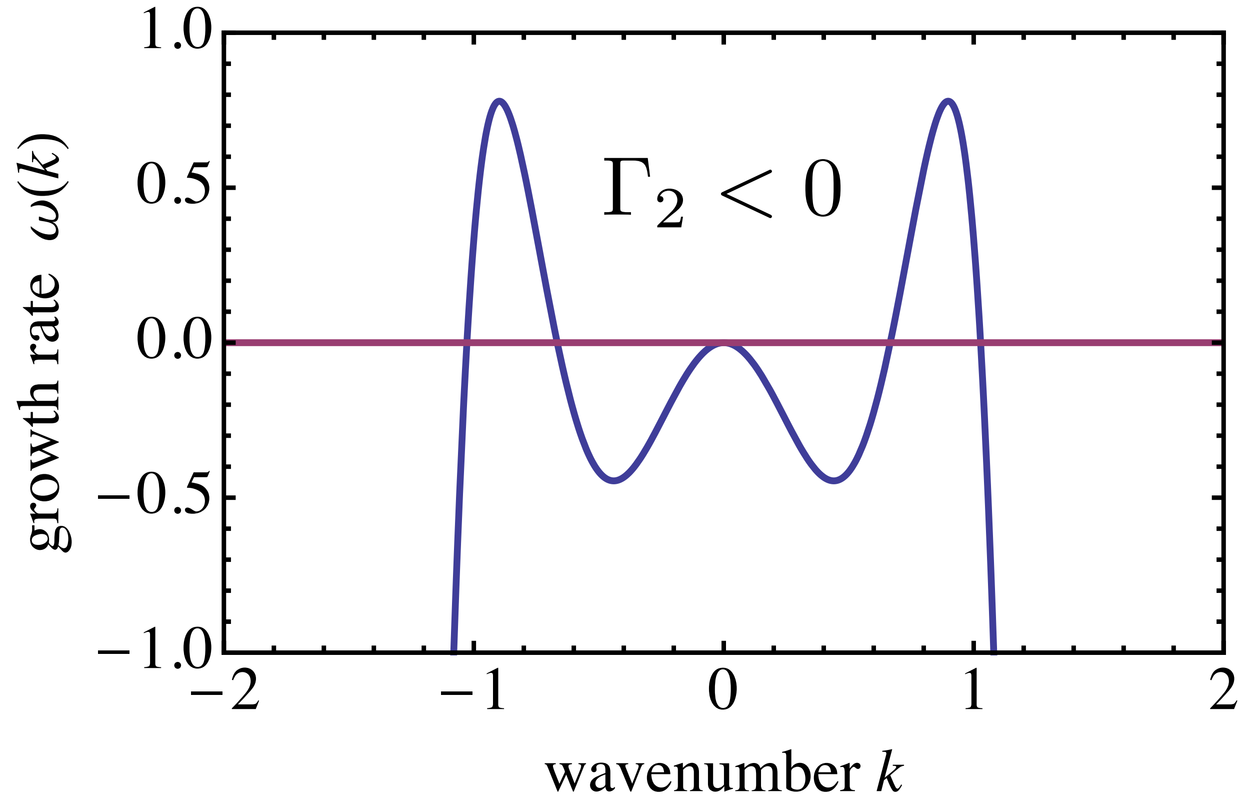

linear stability

Minimal momentum-conserving model

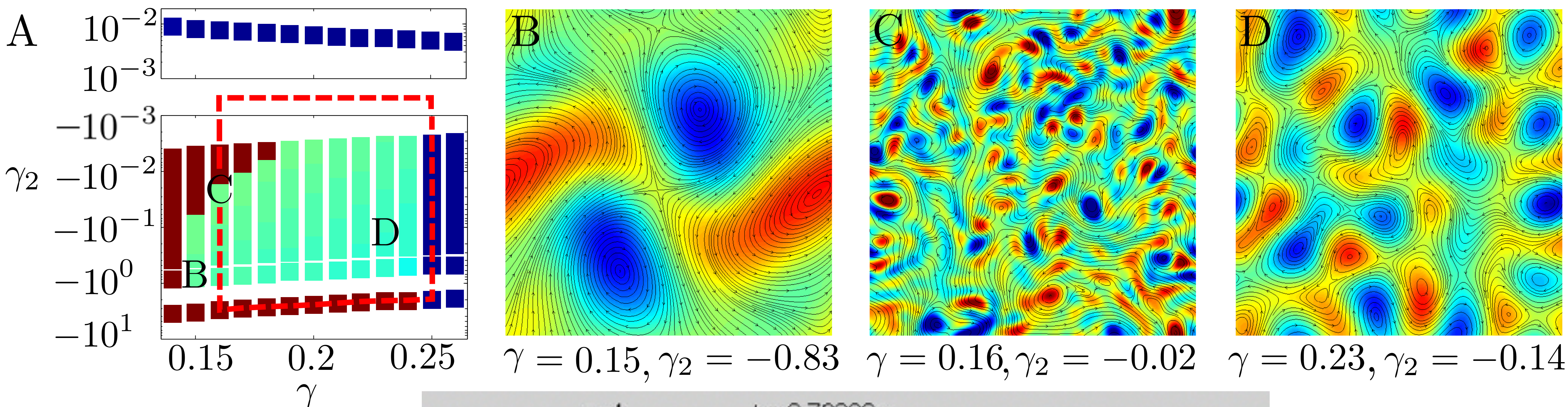

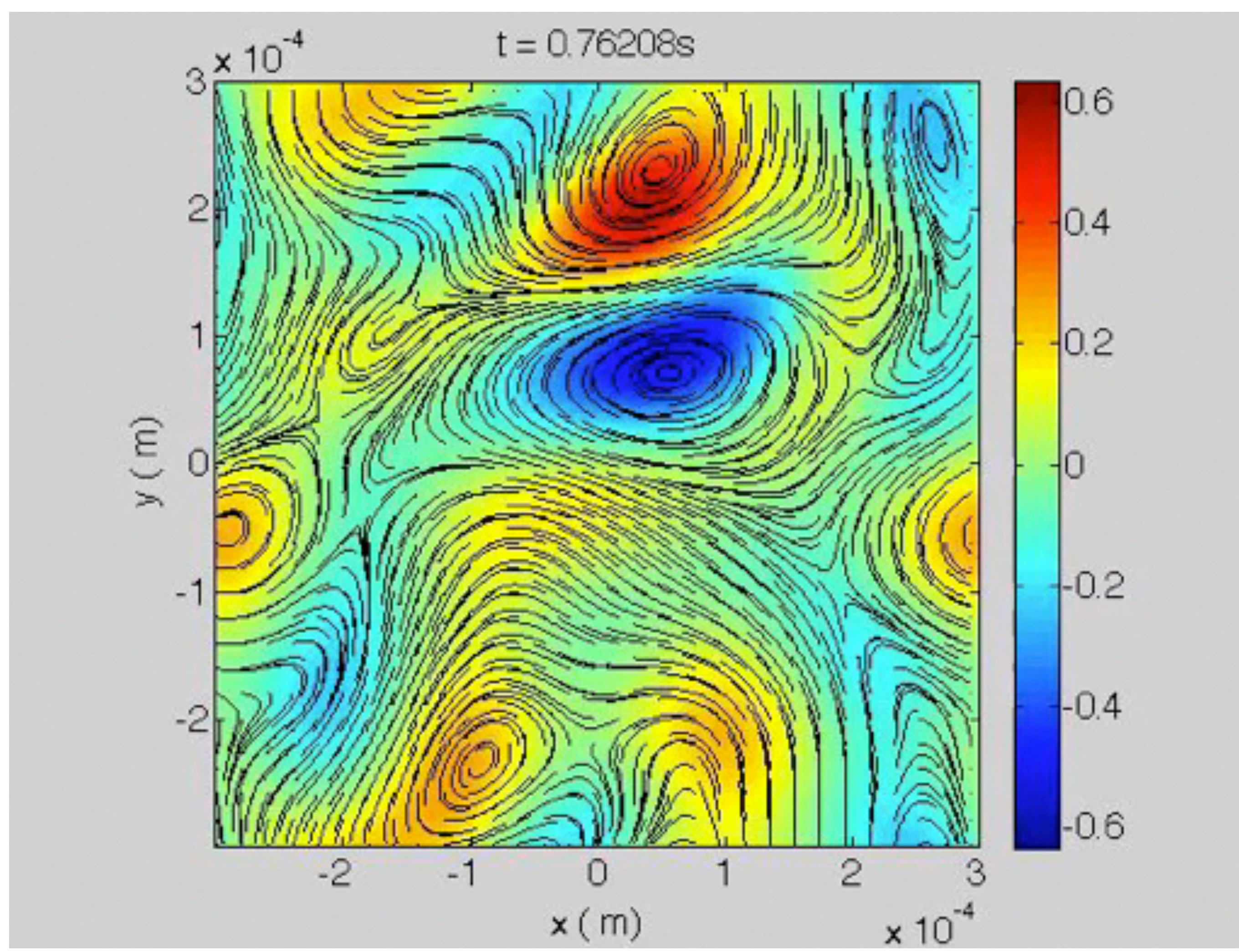

Minimal momentum-conserving model for solvent flow

Flow equations

$$\begin{aligned} 0 &= \nabla \cdot \boldsymbol{v} \\ \partial_t \boldsymbol{v} + (\boldsymbol{v} \cdot \nabla)\boldsymbol{v} &= -\nabla p + \nabla \cdot \boldsymbol{\sigma} \end{aligned}$$

with stress tensor

$$\boldsymbol{\sigma} = [\Gamma_0 - \Gamma_2(\nabla^2) + \Gamma_4(\nabla^2)^2](\nabla^\top \boldsymbol{v} + \nabla \boldsymbol{v}^\top)$$

6th order PDE

S-type: First and second-order derivatives vanish.
W-type: Second and fourth-order derivatives vanish.

Preliminary numerical results

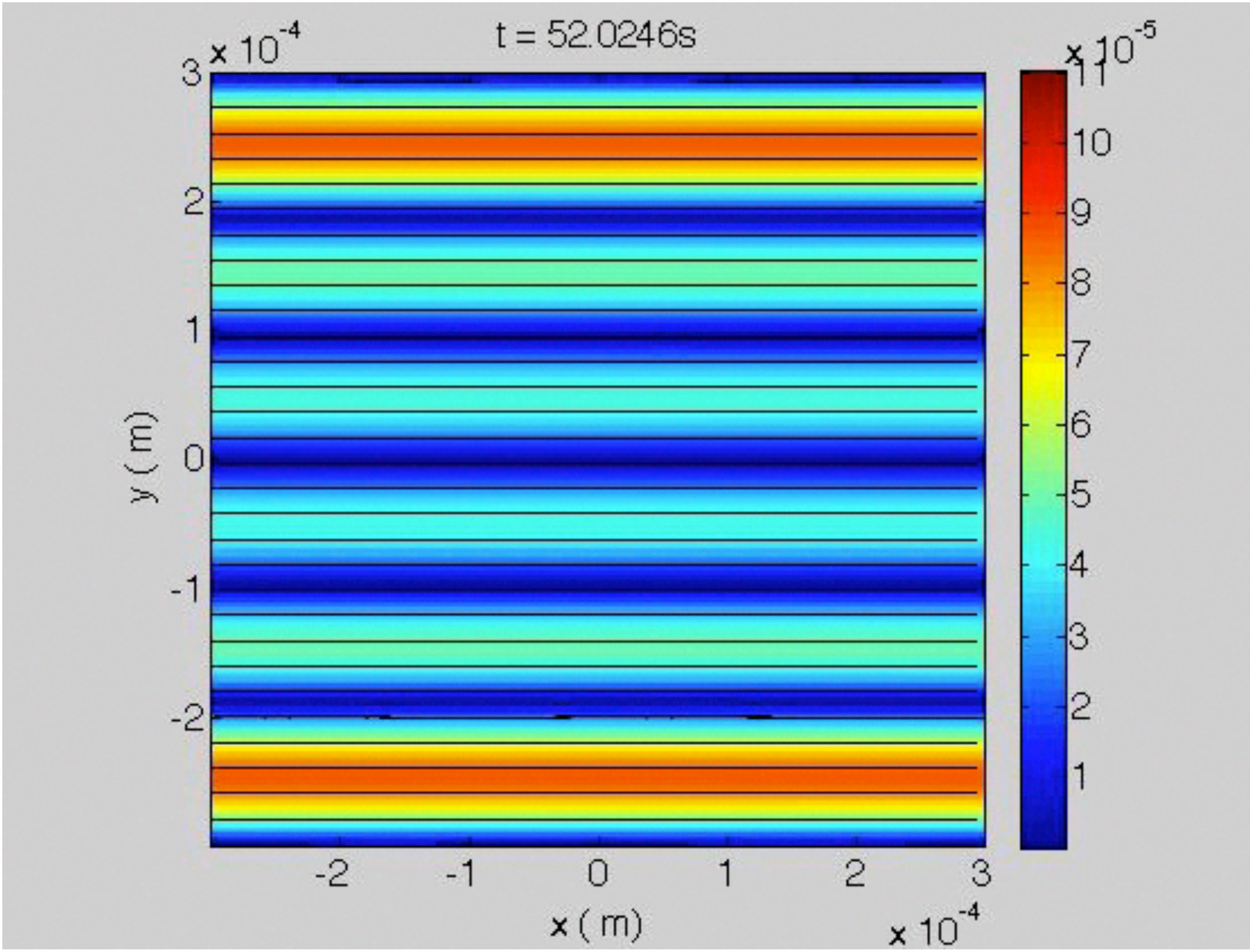

Active nematics

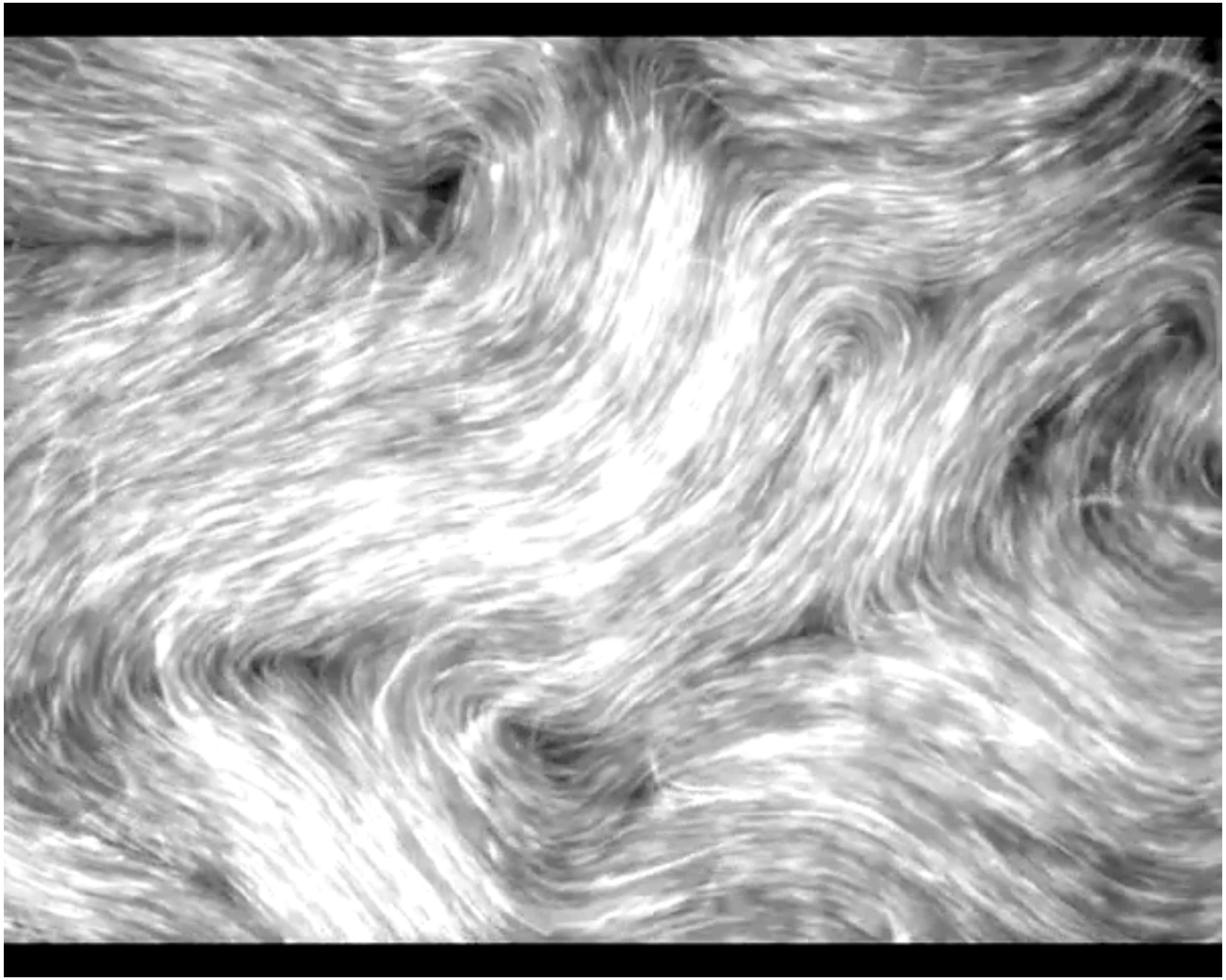

Dogic lab (Brandeis) Nature 2012

Active nematics

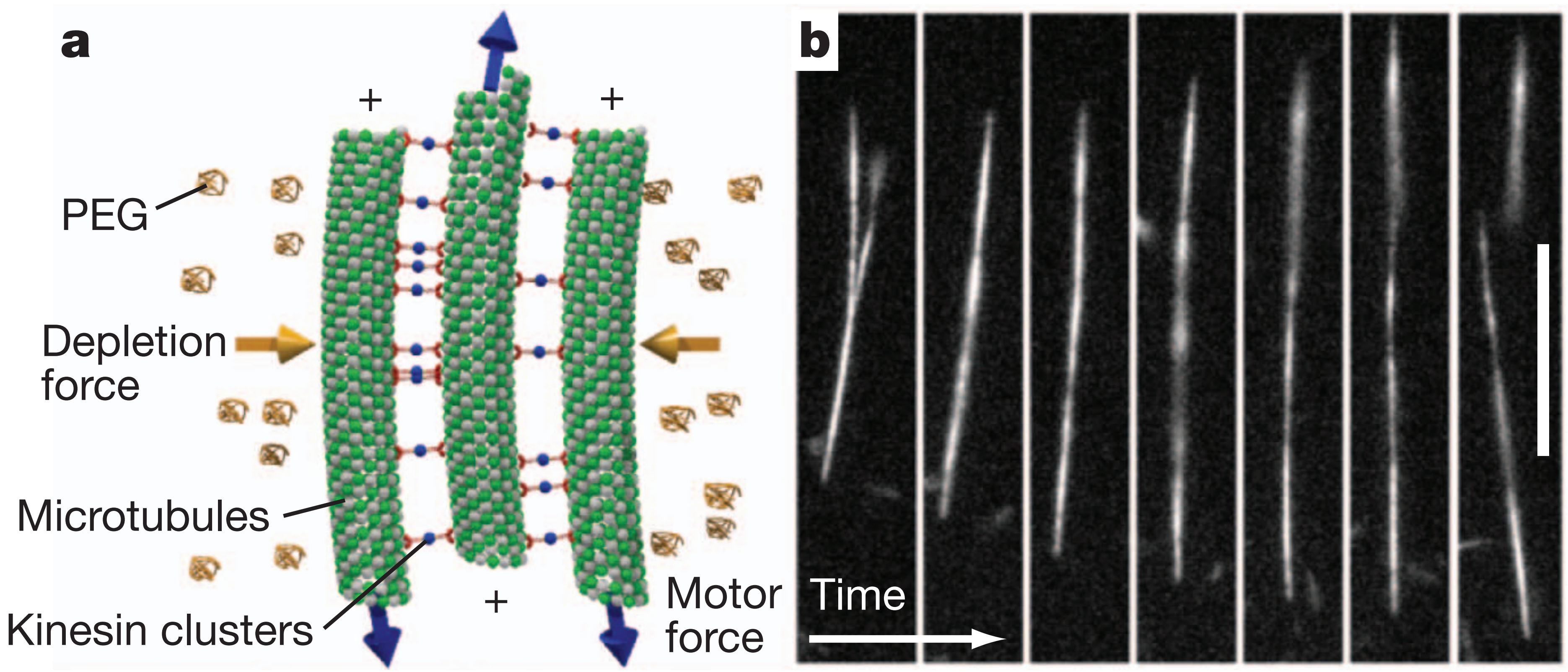

Dogic lab (Brandeis) Nature 2012

no head or tail ⇒ Q-tensor order-parameter

$$Q_{ij} = Q_{ji}\ , \qquad \mathrm{Tr}\, Q = 0 \qquad Q = \begin{pmatrix} \lambda & \mu \\ \mu & -\lambda \end{pmatrix} .$$

$$\Delta = \sqrt{\lambda^2 + \mu^2}, \qquad \Lambda^{\pm} = \pm\Delta$$

Standard model

$$u_{ij} = (\partial_i v_j + \partial_j v_i)/2$$

$$\omega_{ij} = (\partial_i v_j - \partial_j v_i)/2$$

$$D_{ij} = D_0 \delta_{ij} + D_1 Q_{ij}$$

$$\frac{Dc}{Dt} = \partial_i [D_{ij} \partial_j c + \alpha_1 c^2 \partial_j Q_{ij}],$$

$$\rho \frac{Dv_i}{Dt} = \eta \nabla^2 v_i - \partial_i p + \partial_j \sigma_{ij},$$

$$\frac{DQ_{ij}}{Dt} = \lambda S u_{ij} + Q_{ik}\omega_{kj} - \omega_{ik} Q_{kj} + \gamma^{-1} H_{ij},$$

$$\nabla \cdot \boldsymbol{v} = 0,$$

$$H_{ij} = -\delta F/\delta Q_{ij},$$

$$F/K = \int dA \left[\frac{1}{4}(c - c^\star)\mathrm{tr}\boldsymbol{Q}^2 + \frac{1}{4}c(\mathrm{tr}\boldsymbol{Q}^2)^2 + \frac{1}{2}|\nabla \boldsymbol{Q}|^2\right],$$

Giomi et al PRL 2012

Active nematics

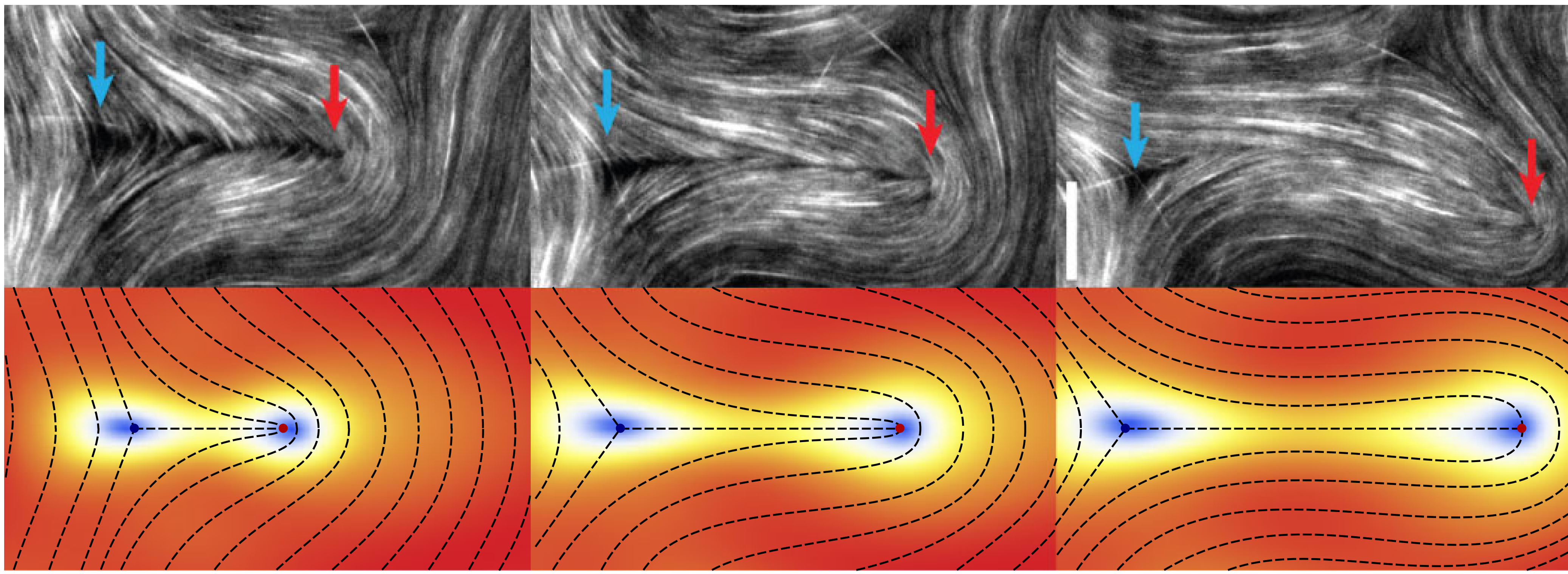

$\boxed{\nabla \cdot \boldsymbol{v} = 0,}$

not consistent with experimental setup

Giomi et al PRL 2012

Turing pattern

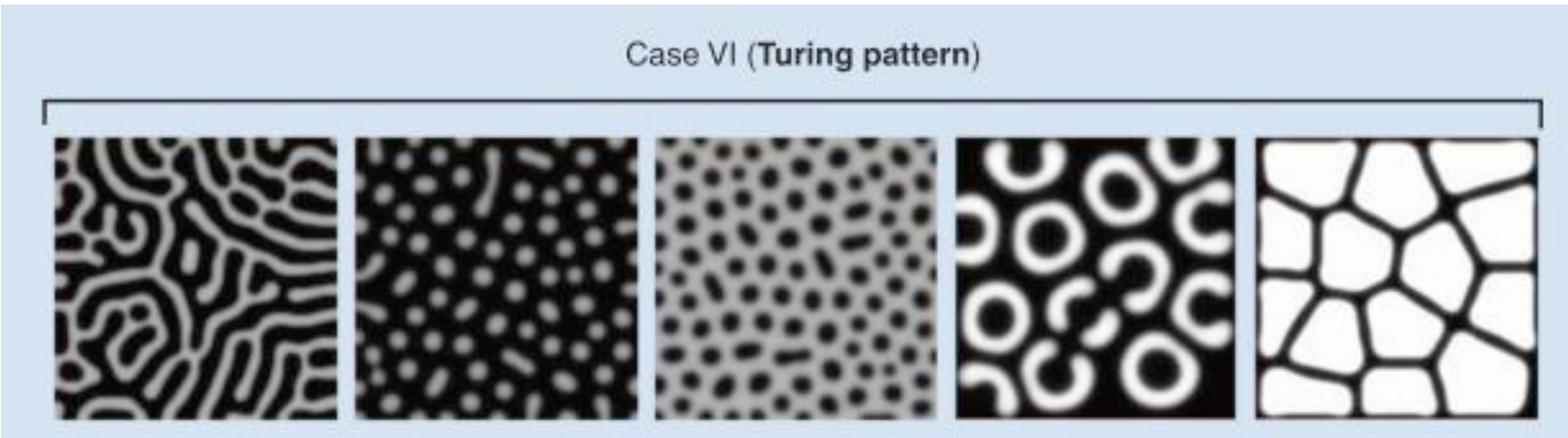

Kondo S, & Miura T (2010). Reaction-diffusion model as a framework for understanding biological pattern formation. *Science, 329* (5999), 1616-20

The matching of zebrafish stripe formation and a Turing model

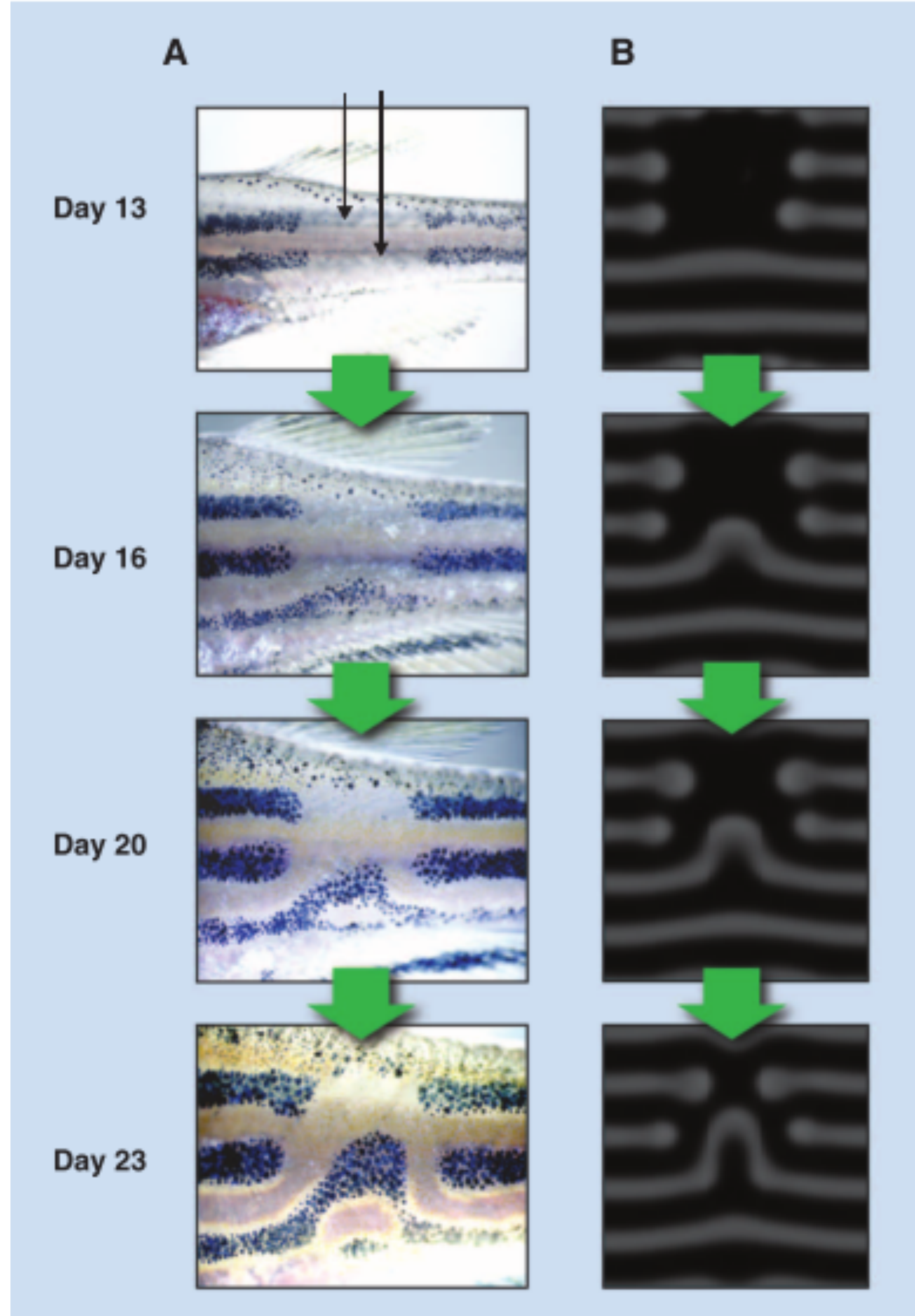

Kondo S, & Miura T (2010). Reaction-diffusion model as a framework for understanding biological pattern formation. *Science, 329* (5999), 1616-20

dunkel@math.mit.edu

4.4 Reaction-diffusion systems (RDSs)

RDSs constitute a class of generic mathematical models of structure formation, which can represented in the form

$$\partial_t \boldsymbol{q}(t, \boldsymbol{x}) = D\nabla^2 \boldsymbol{q} + \boldsymbol{R}(\boldsymbol{q}), \tag{4.39}$$

where

- $q(t, \boldsymbol{x})$ as an n-dimensional vector field describing the concentrations of n chemical substances, species etc.
- D is a *diagonal* $n \times n$-diffusion matrix, and
- the n-dimensional vector $\boldsymbol{R}(\boldsymbol{q})$ accounts for all *local* reactions.

4.4.1 One-dimensional examples

Assuming $\boldsymbol{q}(t, \boldsymbol{x}) = u(t, x)$, the class of one-dimensional RDSs

$$u_t = D u_{xx} + R(u), \tag{4.40}$$

includes the following well-known models:

(i) Fisher's equation [Fis30]

$$R(u) = \alpha\, u(u_0 - u)\ , \qquad \alpha > 0, u_0 > 0 \tag{4.41a}$$

originally proposed to describe the spreading of biological species.

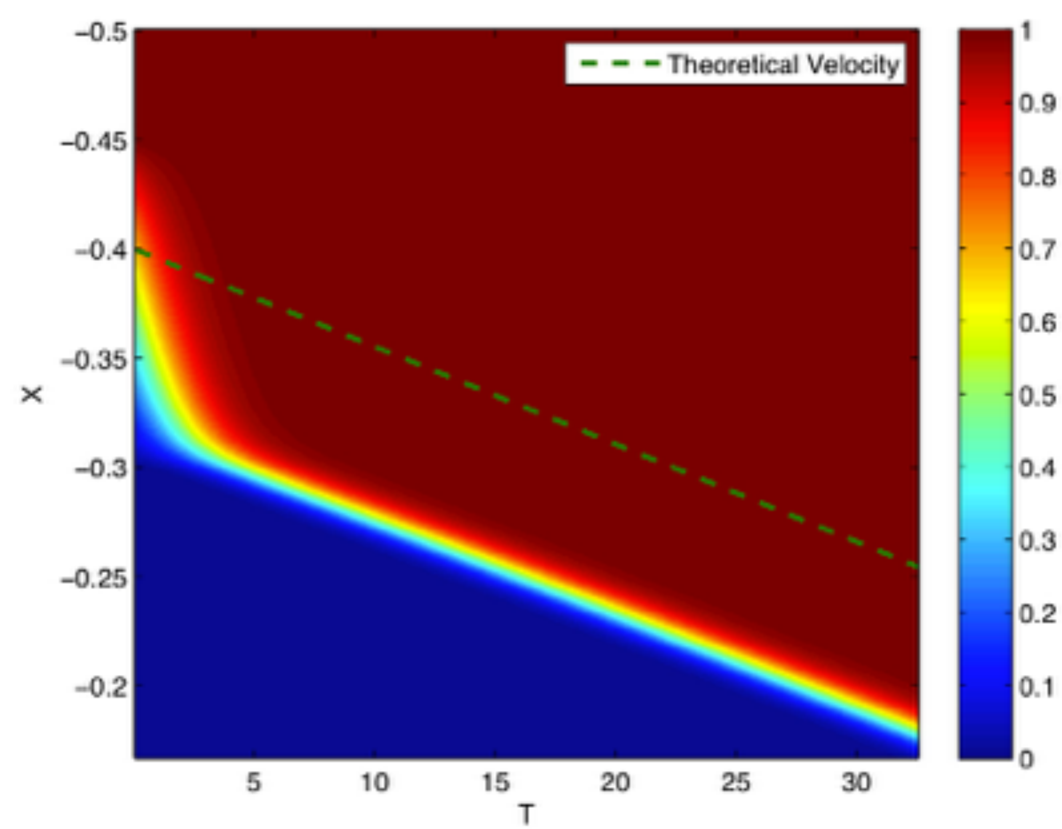

wiki

dunkel@math.mit.edu

4.4.1 One-dimensional examples

Assuming $\boldsymbol{q}(t,\boldsymbol{x}) = u(t,x)$, the class of one-dimensional RDSs

$$u_t = D u_{xx} + R(u), \tag{4.40}$$

includes the following well-known models:

(i) Fisher's equation [Fis30]

$$R(u) = \alpha\, u(u_0 - u)\ , \qquad \alpha > 0, u_0 > 0 \tag{4.41a}$$

originally proposed to describe the spreading of biological species.

(ii) The Newell-Whitehead-Segel equation

$$R(u) = \beta\, u(u_0^2 - u^2)\ , \qquad \beta > 0, \tag{4.41b}$$

which provides an effective description of Rayleigh-Benard convection.

(iii) The Zeldovich equation

$$R(u) = \beta\, u(u_0 - u)(u - a)\ , \qquad \beta > 0, u_0 > a > 0, \tag{4.41c}$$

which arises in combustion theory.

4.4.1 One-dimensional examples

Assuming $\boldsymbol{q}(t, \boldsymbol{x}) = u(t, x)$, the class of one-dimensional RDSs

$$u_t = Du_{xx} + R(u), \tag{4.40}$$

includes the following well-known models:

A rather generic feature of RDSs is that they admit wave-like solutions when complemented with suitable boundary conditions. As an example, consider the Fisher equation (4.41a), which after rescaling of (t, x, u), can be rewritten as

$$u_t = u_{xx} + u(1-u). \tag{4.42}$$

Looking for travelling wave solutions

$$u(t, x) = w(z)\ , \qquad z = x - ct, \tag{4.43a}$$

and using

$$u_t = \frac{dw}{dz}\frac{dz}{dt} = -cw'\ , \qquad u_x = \frac{dw}{dz}\frac{dz}{dx} = w'\ , \qquad u_{xx} = w'' \tag{4.43b}$$

dunkel@math.mit.edu

$$u_t = u_{xx} + u(1-u) \qquad u(t,x) = w(z)\ , \qquad z = x - ct,$$

we may rewrite (4.42) as

$$w'' + cw' + w(1-w) = 0. \tag{4.44a}$$

One can show [AZ79] that, for every wave-speed $c \geq 2$, Eq. (4.44a) possesses solutions $w(z)$ that satisfy

$$\lim_{z\to-\infty} w(z) = 1\ , \qquad \lim_{z\to+\infty} w(z) = 0. \tag{4.44b}$$

Note that these solutions interpolate between the two fixed points $u = 1$ and $u = 0$. No such solution exists for $c < 2$, and for $c \geq 2$ the exact shape of the wave depends on the value of c. Closed analytical solutions can be found for the particular value $c = 5/\sqrt{6}$; in this case [AZ79]

$$w(z) = \frac{1}{\left[1 + r\exp(z/\sqrt{6})\right]^2} \tag{4.44c}$$

for all $r > 0$.

4.4.2 Two species in one space dimension

As a slightly more complex case, let us now consider $\boldsymbol{q}(t,\boldsymbol{x}) = (u(t,x), v(t,x))$, $D = \mathrm{diag}(D_u, D_v)$ and $\boldsymbol{R} = (F(u,v), G(u,v))$, then

$$
\begin{aligned}
u_t &= D_u u_{xx} + F(u,v) && (4.45\text{a})\\
v_t &= D_v v_{xx} + G(u,v) && (4.45\text{b})
\end{aligned}
$$

In general, (F, G) can be derived from the reaction/reproduction kinetics, and conservation laws may impose restrictions on permissible functions (F, G). The fixed points (u_*, v_*) of (4.45) are determined by the condition

$$
\boldsymbol{R}(u_*, v_*) = \begin{pmatrix} F(u_*, v_*) \\ G(u_*, v_*) \end{pmatrix} = \mathbf{0}. \tag{4.46}
$$

Expanding (4.45) for small plane-wave perturbations

$$
\begin{pmatrix} u(t,x) \\ v(t,x) \end{pmatrix} = \begin{pmatrix} u_* \\ v_* \end{pmatrix} + \boldsymbol{\epsilon}(t,x) \tag{4.47a}
$$

with

$$
\boldsymbol{\epsilon} = \hat{\boldsymbol{\epsilon}}\, e^{\sigma t - ikx} = \begin{pmatrix} \hat{\epsilon} \\ \hat{\eta} \end{pmatrix} e^{\sigma t - ikx}, \tag{4.47b}
$$

we find the linear equation

$$
\sigma \hat{\boldsymbol{\epsilon}} = -\begin{pmatrix} k^2 D_u & 0 \\ 0 & k^2 D_v \end{pmatrix} \hat{\boldsymbol{\epsilon}} + \begin{pmatrix} F_u^* & F_v^* \\ G_u^* & G_v^* \end{pmatrix} \hat{\boldsymbol{\epsilon}} \equiv M \hat{\boldsymbol{\epsilon}}, \tag{4.48}
$$

where

$$
F_u^* = \partial_u F(u_*, v_*)\ , \qquad F_v^* = \partial_v F(u_*, v_*)\ , \qquad G_u^* = \partial_u G(u_*, v_*)\ , \qquad G_v^* = \partial_v G(u_*, v_*).
$$

we find the linear equation

$$\sigma\hat{\boldsymbol{\epsilon}} = -\begin{pmatrix} k^2 D_u & 0 \\ 0 & k^2 D_v \end{pmatrix} \hat{\boldsymbol{\epsilon}} + \begin{pmatrix} F_u^* & F_v^* \\ G_u^* & G_v^* \end{pmatrix} \hat{\boldsymbol{\epsilon}} \equiv M\hat{\boldsymbol{\epsilon}}, \tag{4.48}$$

where

$$F_u^* = \partial_u F(u_*, v_*) \ , \qquad F_v^* = \partial_v F(u_*, v_*) \ , \qquad G_u^* = \partial_u G(u_*, v_*) \ , \qquad G_v^* = \partial_v G(u_*, v_*).$$

Solving this eigenvalue equation for σ, we obtain

$$\sigma_\pm = \frac{1}{2}\left\{ -(D_u + D_v)k^2 + (F_u^* + G_v^*) \pm \sqrt{4F_v^* G_u^* + [F_u^* - G_v^* + (D_v - D_u)k^2]^2} \right\}, \tag{4.49}$$

which gives

$$\det M = \sigma_+\sigma_- = (F_u^* - D_u k^2)(G_v^* - D_v k^2) - F_v^* G_u^*, \tag{4.50a}$$

$$\operatorname{tr} M = \sigma_+ + \sigma_- = F_u^* + G_v^* - (D_u + D_v)k^2. \tag{4.50b}$$

In order to have an instability for some finite value k, at least one of the two eigenvalues must have a positive real part. If the eigenvalues are real, this means that either the condition

$$\det M < 0, \tag{4.51a}$$

or the conditions

$$\det M > 0 \quad \wedge \quad \operatorname{tr} M > 0 \tag{4.51b}$$

must be satisfied. These criteria can be easily tested for a given reaction kinetics (F, G). We briefly summarize two popular examples.

Lotka-Volterra model This model describes a simple predator-prey dynamics, defined by

$$F(u,v) = Au - Buv, \tag{4.52a}$$
$$G(u,v) = -Cv + Euv \tag{4.52b}$$

with positive rate parameters $A, B, C, E > 0$. The field $u(t,x)$ measures the concentration of prey and $v(t,x)$ that of the predators. The model has two fixed points

$$(u_0, v_0) = (0,0)\ , \qquad (u_*, v_*) = (C/E, A/B), \tag{4.53}$$

with Jacobians

$$\begin{pmatrix} F_u(u_0,v_0) & F_v(u_0,v_0) \\ G_u(u_0,v_0) & G_v(u_0,v_0) \end{pmatrix} = \begin{pmatrix} A & 0 \\ 0 & -C \end{pmatrix} \tag{4.54a}$$

and

$$\begin{pmatrix} F_u(u_*,v_*) & F_v(u_*,v_*) \\ G_u(u_*,v_*) & G_v(u_*,v_*) \end{pmatrix} = \begin{pmatrix} A - \frac{BC}{E} & -A \\ C & -C + \frac{AE}{B} \end{pmatrix}. \tag{4.54b}$$

It is straightforward to verify that, for suitable choices of A, B, C, D, the model exhibits a range of unstable k-modes.

FitzHugh-Nagumo model This model aims to describe the propagation of an action potential through nerve cells, and is defined by

$$F(u,v) = \lambda u - \mu u^3 - \eta v + \kappa, \tag{4.55a}$$

$$G(u,v) = \frac{1}{\tau}(u - \beta v) \tag{4.55b}$$

with positive parameters $\lambda, \mu, \tau, \eta, \beta$. The field $u(t,x)$ measures the membrane voltage, and $v(t,x)$ is a slower gate voltage that controls relaxation of u. The parameter κ represents external currents that cause an increase of u. Similar to the Lotka-Volterra model, the FitzHugh-Nagumo model exhibits a range of unstable k-modes for biologically relevant parameters choices.

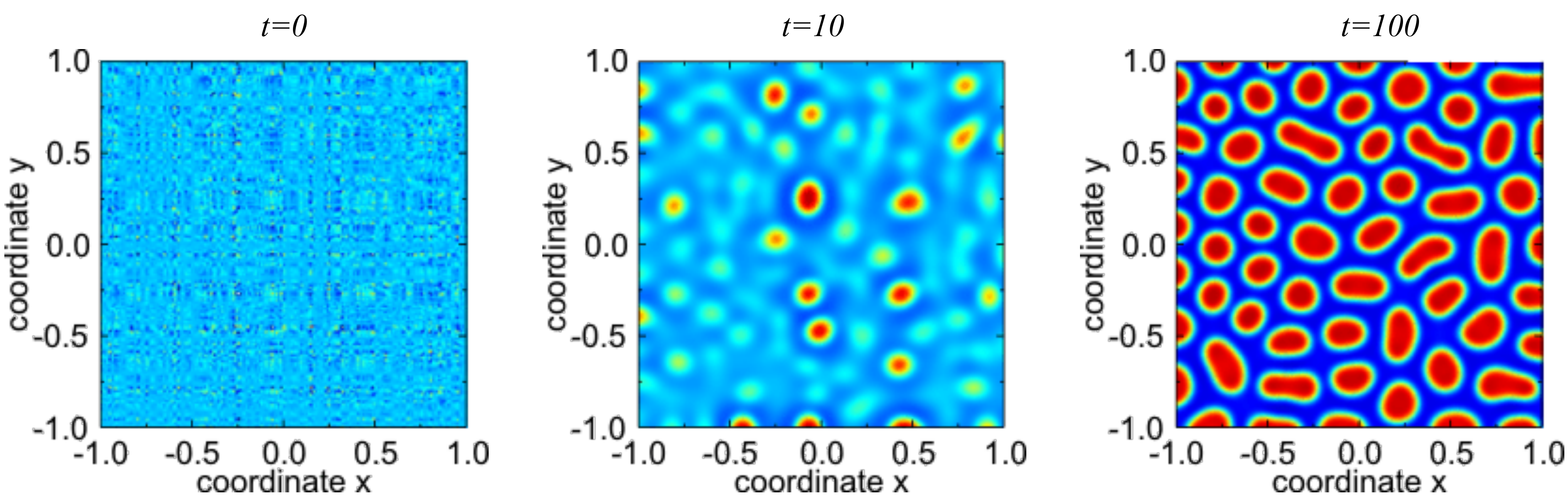

FitzHugh-Nagumo model This model aims to describe the propagation of an action potential through nerve cells, and is defined by

$$F(u, v) = \lambda u - \mu u^3 - \eta v + \kappa, \tag{4.55a}$$

$$G(u, v) = \frac{1}{\tau}(u - \beta v) \tag{4.55b}$$

with positive parameters $\lambda, \mu, \tau, \eta, \beta$. The field $u(t, x)$ measures the membrane voltage, and $v(t, x)$ is a slower gate voltage that controls relaxation of u. The parameter κ represents external currents that cause an increase of u. Similar to the Lotka-Volterra model, the FitzHugh-Nagumo model exhibits a range of unstable k-modes for biologically relevant parameters choices.

other possible states in FitzHugh-Nagumo-type models

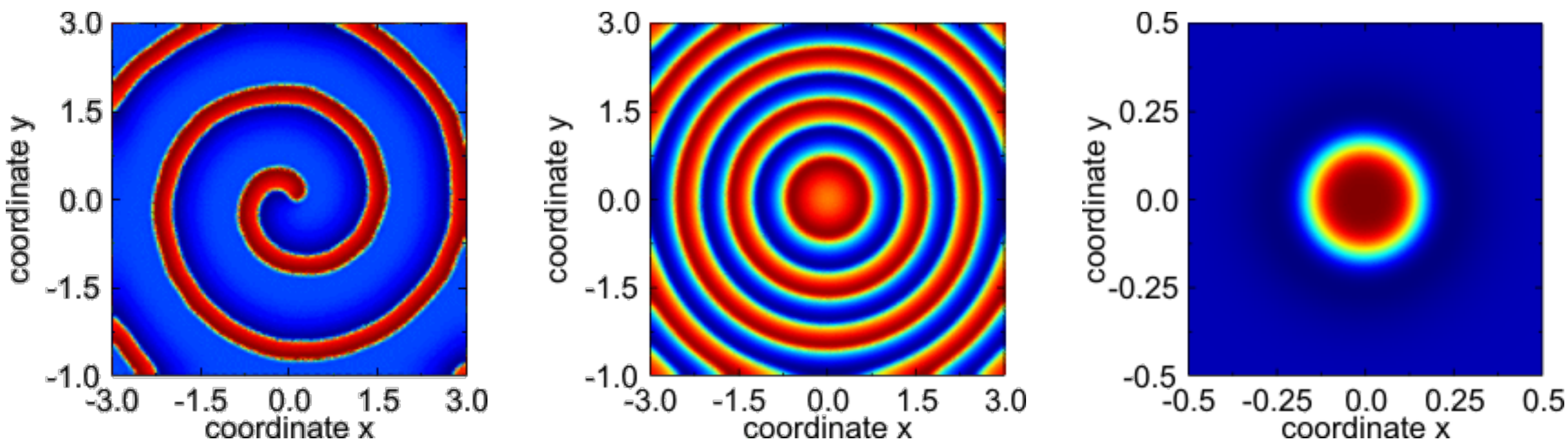

dunkel@math.mit.edu